Case Studies in Construction Materials 19 (2023) e02400

Contents lists available at ScienceDirect

Case Studies in Construction Materials

journal homepage: www.elsevier.com/locate/cscm

Optimisation of compressive strength of foamed concrete with a novel Aspergillus iizukae EAN605 fungus

Honin Ali Yahya Alshaeer [a,*], J.M. Irwan [a,*], Abdullah Faisal Alshalif [a,*], Efaq Ali Noman [b], Mugahed Amran [d,e], Yaser Gamil [f,g,**], Abdulmajeed Alhokabi [h], Adel Ali Al-Gheethi [c]

[a] Jamilus Research Centre for Sustainable Construction (JRC-SC), Faculty of Civil Engineering and Built Environment, Universiti Tun Hussein Onn Malaysia, Parit Raja, 86400 Johor, Malaysia
[b] Department of Applied Microbiology, Faculty of Applied Sciences, Taiz University, Taiz, Yemen
[c] Global Centre for Environmental Remediation (GCER), University of Newcastle and CRC for Contamination Assessment and Remediation of the Environment (CRC CARE), Newcastle, Australia
[d] Department of Civil Engineering, College of Engineering, Prince Sattam Bin Abdulaziz University, 11942 Alkharj, Saudi Arabia,
[e] Department of Civil Engineering, Faculty of Engineering and IT, Amran University, 9677 Amran, Yemen
[f] Building materials, Department of Civil, Environmental and Natural Resources Engineering, Luleå University of Technology, Sweden
[g] Department of Civil Engineering, School of Engineering, Monash University Malaysia, Jalan Lagoon Selatan, 47500 Bandar, Sunway, Selangor, Malaysia
[h] Department of Civil Engineering, Faculty of Engineering, University of Malaya, 50603 Kuala Lumpur, Malaysia

ARTICLE INFO

Keywords:
Biofoam concrete
Foamed concrete
Aspergillus iizukae EAN605
Calcium carbonate, Compressive strength

ABSTRACT

The production of concrete by incorporating a microorganism has emerged as a promising research area, offering potential benefits such as reduce carbon footprint, enhance durability and increased strength. The present study reported for the first time using a fungal strain *(Aspergillus iizukae EAN605)* in biocementation. The study aims to investigate the effectiveness of incorporating *Aspergillus iizukae EAN 605* into foam concrete to improve its performance, particularly its strength. The study employs the response surface methodology (RSM) to explore the relationship between density, microorganism concentration and water /cement ratio (w/c) and their effects on compressive strength. Through a series of experiments,the highest recorded compressive strength was achieved with a density of 1800 kg/m^3, w/c ratio of 0.5, and Aspergillus iizukae EAN605 concentration of 0.5 g/l, resulting in a remarkable 37.5 % increase compared to foam concrete (FC). The variables of density, *A. iizukae* EAN 605 and their interaction density*fungi (D*F) significantly impacted compressive strength, with p-values of 0.000, 0.016, and 0.010, respectively.X-ray diffraction (XRD) analysis was employed to identify the crystalline composition of the precipitates formed on the fungal hyphae, providing insights into the mineralogical transformations occurring during the biocementation process. Additionally, scanning electron microscope (SEM) imaging was utilised to visualise the morphology and distribution of the calcite crystals, further supporting the evidence of fungal-mediated mineral precipitation in foam concrete. The findings of this study hold significant implications for the concrete industry, as the

* Corresponding authors.
** Corresponding author at: Building materials, Department of Civil, Environmental and Natural Resources Engineering, Luleå University of Technology, Sweden.
E-mail addresses: honinalshaeer99@gmail.com (H.A.Y. Alshaeer), irwan@uthm.edu.my (J.M. Irwan), faisalalshalif@gmail.com (A.F. Alshalif), yaser.gamil@ltu.se (Y. Gamil).

https://doi.org/10.1016/j.cscm.2023.e02400
Received 11 May 2023; Received in revised form 7 August 2023; Accepted 13 August 2023
Available online 15 August 2023

incorporation of Aspergillus iizukae EAN605 in foam concrete offers a sustainable solution to enhance compressive strength and contribute to environmental friendly construction practices. This study provides valuable insights for future research and practical applications in the field of bio-foamed concrete (B-FC).

1. Introduction

Foamed concrete (FC) is a lightweight and porous material that has gained popularity in construction due to its excellent insulation, high porosity, low density, and sound absorption properties [1–6]. Other benefits such as self-compacting, excellent workability, ease of fabrication, durability and cost effectiveness have been highlighted in previous studies [7–9]. One significant parameter to address is the performance of FC in respect to its characterstic strength [10–14]. The strength is influenced by various factors, including the types of cementitious materials used, the amount of cement, the proportions of the mixture, the water-cement ratio, the volume of foam, the foaming agent, the curing method, and the presence of additives [15–18]. The use of foam in the concrete mixture creates a matrix of air bubbles, which reduces the density of the material and enhances its thermal insulation capabilities compared to traditional dense concrete [19–21]. It is important to regulate a balance between strength and density, aiming to maximize strength. According to Visagie and Kearsley [22], the compressive strength of foam concrete does not appear to be affected by the distribution of air voids at higher densities. This observation may be attributed to a more even distribution of air voids at higher densities. Relatively, Luping [23] noted that larger pores have a greater impact on concrete strength compared to smaller pores. It is also reported that when comparing materials with the same matrix and porosity, the strength tends to be lower in the presence of a higher concentration of larger-sized pores [24–28].

However, despite its many benefits, one of the main challenges in producing FC is achieving optimal mechanical properties [29]. The reason is that FC has more pores and is more susceptible to temperature changes, moisture, humidity, and issues like shrinkage, which can cause cracking, freezing, thawing, chemical damage, and other types of wear and tear which then leads to decrease compressive strength and stiffness [30–32]. According to [33], durability studies have shown that the cell-like structure and potential porosity of foam concrete (FC) do not make it less resistant to the penetration of aggressive ions compared to densely compacted normal weight concrete. This is attributed to the lower ratio of connected pores to total pores in FC, which plays a crucial role in determining durability. Several experimental models have been proposed to establish a relationship between porosity and strength of porous materials. Some models have specifically focused on relating strength to porosity in FC [8]. The study by Kumara and Bhattacharjeeb [34], have examined the pore system and introduced a new model that takes into account various factors such as porosity, pore size distribution, cement content, aggregate type, exposure conditions, and age of the concrete. They discovered that the existing models that relate strength to pore size characteristics in cement-based materials were insufficient in providing a proper explanation. Furthermore, it has been observed that the distribution of air voids in FC is more uniform at a lower dosage of foam volume compared to a higher foam volume content. This uniformity holds true for FC mixes containing fly ash compared to concrete mixes composed only of sand [35]. Studies have also shown that the plastic density of FC increases proportionally with an increase in the water-to-cement ratio and a decrease in the foam concentration [36]. The mix proportion, density, and compressive strength of FC

Table 1
A summary of the mix proportion, density, and compressive strength of FC as reported by previous studies.

Refs.	Proportion of cement (kg/m^3) or composition	Density (kg/m^3)	Ratios				Compressive strength (28 days)
			W/C	S/C	F/C	FA/C	
[62]	Cement–sand mix	400–1600	-	-	-	-	0.5–10
[63]	Cement–fly ash replacement (193–577)	1000–1500	0.6–1.17	-		-	2–18
[64]	Neat cement (149–420)	490–660	0.4–0.45	-		-	0.71–2.07
	Cement–sand/fly ash (57–149)		0.5–0.57				0.23–1.1
[33]	300	1000–1400	0.5	1.83–3.17	-	-	1–2
			1.11–1.56		1.22–2.11		3.9–7.3
[33]	500	1400–1800	0.3	1.5–2.3	-	-	10–26
			0.65–0.83		1.15–1.77		20–43
[65]	Cement–sand–fly ash mix	800–1350	With filler–cement ratio varied from 1 to 3 and fly ash replacement for sand varied from 0 % to 100 %				1–7
	Cement–sand mix (fine)	800–1350					2–11
		650–1200					4–19
[33]	OPC and fine sand	650–1200	0–100 %	1–3	-	1–3	2.0–11
[66]	Silica fume and PP fibre	800–1500	0.30–0.60	1–1.61	-	-	39.6–91.3
[67]	Cement-sand concrete sludge	1837	0.5	-	-	-	> 25
[68]	High-strength FC reinforced with polypropylene fibre	800–1500	Fi/C	-	-	0.2–0.76	10–50
[69]	Fly ash, lime, and PP fibre	1000	0.45–1.0	1.5–2.1	-	-	1.6–4.6
[6]	OPC (500 kg/m^3) and lightweight aggregate	1400–1800	0.5–0.6	-	-	-	13.8–48
[70]	Partial replacement (F/C)	1400–1800	0.63–0.83	1.5–2.3	-	1.15–1.78	20–43
[69]	Cementation material, fly ash (10–50 %)	1500–1800	0.3	0.5	-	< 0.25	3.9–10.5

Annotations: W/C: water/cement; Fi/C: filler/cement; FA/C: fly ash/cement; S/C: sand/cement; PP fibre: polypropylene fibre

summarised as reported by previous studies are presented in Table 1.

Enhancing the FC performance through strengthening by fungi is a noteworthy accomplishment. It highlights the potential of utilising biological means to improve the properties of construction materials, particularly in terms of sustainability and durability [37]. FC usage in construction is well-known for its lightweight and insulation properties [33,38,39]. In this study, a new approach was proposed to enhance the strength of FC by incorporating a novel strain of fungus *Aspergillus iizukae* EAN605. The strain of fungus was mixed with cement, water, sand and foam to create bio-foamed concrete (B-FC). The reaction between the fungal strain and other components forms a dense, strong matrix that improves the material's overall properties [40–43]. Microbial reinforcement of cement-based materials offers a sustainable and eco-friendly alternative to traditional reinforcement methods, as it reduces the use of harmful chemicals and contributes to the overall reduction of carbon emissions in the construction industry. This approach also provides concrete buildings with self-healing capabilities [44–46]. Despite the advancements in research on bacteria-mediated self-healing concrete, the field still faces significant limitations.

Despite the advancements in research on bacteria-mediated self-healing concrete, the field still faces significant limitations.The Table 2 presents a compilation of various previous studies focused on the utilization of bacteria in concrete to enhance its compressive

Table 2
The effect of different kinds of bacteria, bacteria concentration, nutrients, and precipitation morphologyon mechanical properties as reported by previous studies.

reference	Type microorganisms	Microorganisms' concentration	Nutrients	Morphology formation of precipitation	Improvement of compressive strength
[71]	Shewanella anaerobic	10^5/ml cell concentration.	N/A	N/A	The most significant enhancement in compressive strength, reaching 24 MPa, is observed at a cell concentration of 10^5 cells/ml, resulting in a 25 % increase after 28 days.
[72]	Sporosarcina pasteurii	10^3,10^5,10^7 cells/ml	N/A	N/A	The greatest improvement in compressive strength, measuring 25 MPa, 28 MPa, and 26 MPa, leads to an increase of 4.1 %, 20 %, and 8.7 % respectively after 28 days.
[73]	Pasteur's Sporosarcina	2×10^6	Extract from yeast and urea	$CaCO_3$	N/A
[74]	Pasteur's Sporosarcina	10^9 cells/ml	Extract from peptone and beef	$CaCO_3$	The regain ratio of compressive strength exhibited a 130 % increase compared to the plain mortar
[75]	Soil bacteria	N/A	Urea, gypsum, and sugar	Aragonite and Calcite	A maximum increase of 23.49 % in compressive strength was observed after a 28-day curing period.
[76]	* Sporosarcina pasteuri *Sporosarcina ureae	10^6 cells/ml	Extract from yeast, urea, and $CaCO_3$	*Crystals with a relatively denser rhombohedral shape. *Crystals with a relatively scattered rhombohedral shape.	The Sporosarcina pasteurii þ zeolite combination yielded the best results, achieving compressive strengths of 100 MPa (for FF mortar) and 65 MPa (for normal mortar) – approximately 10 % higher than control specimens after 270 days.
[77]	*S. pasteurii *B. sphaericus	N/A	Urea, calcium acetate, and nutrient broth	*Calcite crystals: Rhombohedral shape *Vaterite crystals: Spheroid shape	N/A
[78]	B. sphaericus	N/A	*$CaCI_2$ and urea *Calcium acetate and urea	Calcite, vaterite, and aragonite Calcite, and vaterite	N/A
[79]	S. pasteurii	N/A	Calcium chloride Calcium nitrate Calcium acetate	*Hexahedral crystals *Rough-surfaced hexahedral crystals *Acicular crystals with a small number of spherical and lettuce-like crystals	N/A -
[80]	B. megaterium	20 × 10^5 cfu•ml^−1 30 × 10^5 cfu•ml^−1 40 × 10^5 cfu•ml^−1	———	calcite	A concentration of 30 × 10^5 cfu•ml^−1 was determined to be ideal. The highest grade of bacterial concrete exhibited a 24 % improvement in strength, while the lowest grade showed a 12.8 % increase.
[81]	Sporosarcina pasteurii	The concentration of the urea-$CaCI_2$ solution used was 0.2 M.	Solution of urea and calcium chloride ($CaCI_2$)	*Vaterite: Flower-shaped clusters with hexagonal $CaCO_3$. *Calcite: Granular clusters of coarse hexagonal $CaCO_3$ at different scales.	N/A -
[82]	B. sphaericus	106 cells•ml-1, 108 cells•ml-1	*water *luria bertania broth	calcium carbonate	Enhancement of specimens with wastewater surpassed that of water and LB.

strength. These studies collectively contribute to our understanding of the effectiveness of bacterial incorporation in concrete. However, the use of bacteria in self-healing concrete is limited because bacteria have low adaptability [47,48] and cannot survive in harsh environments like high pH, extreme temperatures, or dry conditions. The cost of producing bacterial spores under sterile conditions using expensive growth media also causes the application of bacteria-based self-healing concrete financially infeasible [49, 50]. Alternatively, fungi have been explored to replace bacteria in enhancing calcium mineral precipitation in FC, resulting in increased compressive strength in concrete. Due to their mycelial structures and higher biomass, fungi have higher effectiveness for biocementation, making them good biological fibre to enhance the durability of concrete [51,52]. Fungi are also suitable for harsh environments as they can gather nutrients from the air and rainwater and thrive on surfaces such as rocks, cement, and mortar [53,54]. Some fungi, like *Neurospora crassa* and *Candida ethanolica,* have demonstrated high efficiency in forming biominerals through microbial-induced carbonate precipitation [51,55,56]. Thus, fungi can be used as a protective biocoating agent for porous materials by colonising and promoting the formation of biominerals on the surface. Fungi are a better option than bacteria when it comes to improving concrete properties because they can endure under low water activity levels (0.60–0.85) [57]. Some species, including *Fusarium cerealis*, *Pleospora herbarum*, *Mucor hiemalis* and *Aspergillus nidulans,* possess high urease activity and can withstand high alkaline environments [49]. *Aspergillus nidulans* can grow on concrete surfaces and enhance the formation of calcium carbonate, resulting in improved concrete properties such as increased resistance to cracking and enhanced durability over time [56,58]. When fungi species are introduced into concrete and mortar, a significant improvement in the compressive strength of the concrete is observed. In one study, the use of the fungal sample *Trichoderma viride* resulted in a strength of 31 MPa, representing a 37.7 % increase in compressive strength compared to concrete without the fungus after 28 days of curing [59,60]. Another experiment involving the fungal *Aspergillus spp*. showed a 15.6 % increase in compressive strength at 28 days [61]. Additionally, incorporating *Eupenicillium crustaceum* in ordinary concrete led to a 23 % enhancement in compressive strength after 28 days of curing, when compared to the controlled concrete [60]. This research examines the feasibility of adding a new strain of *Aspergillus iizukae* EAN605 to the FC mixture to enhance its performance and longevity without increasing weight. This fungi opens up the possibility of utilising it in other applications, such as repairing cracks in concrete structures through self-healing. The aims of this study is to improve the compressive strength of foam concrete by incorporating A. iizukae EAN605 into its production process.The study evaluates the impact of various concentrations of *A. iizukae* EAN605 on optimising compressive strength over 28 days using response surface methodology (RSM). The purpose of using RSM is to enhance the response of compressive strength by utilising an effective statistical method for optimising and modelling the influence of three factors: density, *Aspergillus iizukae EAN605* concentrations, and water cement ratio w/c. This allows for the prediction of optimal performance with minimal experimentation and aids researchers in finding the optimal conditions.

2. Materials and methods

This study used FC and B-FC, which are lightweight concretes made using a foaming agent to create a mixture of air bubbles and cement. The same materials (cement, fine aggregate, water, and chemical foaming agent) were used for FC, but the incorporation of fungi in FC gave a new material named B-FC. The B-FC has similar properties as FC but is more sustainable, thus considered a green alternative. RSM was employed to optimise the compressive strength of B-FC using fungus.

2.1. Materials

In this study, cement and sand were used as solid materials to create FC and B-FC. Ordinary Portland Cement (OPC) produced by cement industries of Malaysia Berhad (CIMA), which meet the American Society for Testing and Materials (ASTM) Type I and MS 522 standards, was used in the current work [83]. The composition and specifications of the OPC are defined in the British Standard BS 197–1:2000 Table 3 [84]. The amount of cement used in the study was adjusted based on the density of the FC mixture used with and without fungi *(Aspergillus iizukae* EAN605*)*. The natural sand used in this study was obtained from a river and analysed in the material laboratory at Universiti Tun Hussein Onn Malaysia (UTHM) using the particle size distribution method specified in IS 383:1970 [85, 86], as shown in Fig. 2(a,b,c and d). The sand was sieved to retain only the particles that could pass through a 1 mm sieve, which was then used as fine sand in the production of FC and B-FC. To ensure it was free from microbial contamination, the sand was heated at 100 °C for 24 h, as shown in Fig. 1, before being cooled to room temperature and added to the concrete mixture (Fig. 2).

Water and synthetic foaming agents were utilised as the liquid materials to produce FC, and *Aspergillus iizukae* EAN605 was added to create B-FC. Water was used for mixing and curing in FC, and B-FC used clean water from the supplied network. The water was combined with a FC mix to make FC. The same water, adding *A. iizukae* EAN605, was used to produce B-FC. The mixture was stirred to

Tablee 3
Chemical composition of the OPC.

Chemical Compound	Proportion (%)
SiO_2	20.6
Al_2O_3	5.4
Fe_2O_3	4.2
SO_3	2.2
K_2O	0.6
CaO	64.8
MgO	2.2

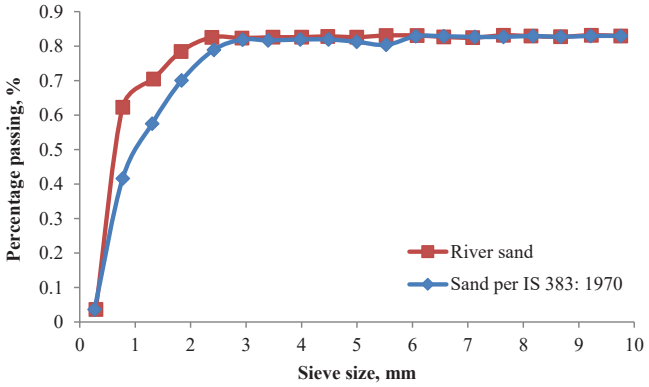

Fig. 1. The grade distribution of river sand (Data adopted from [85,86]).

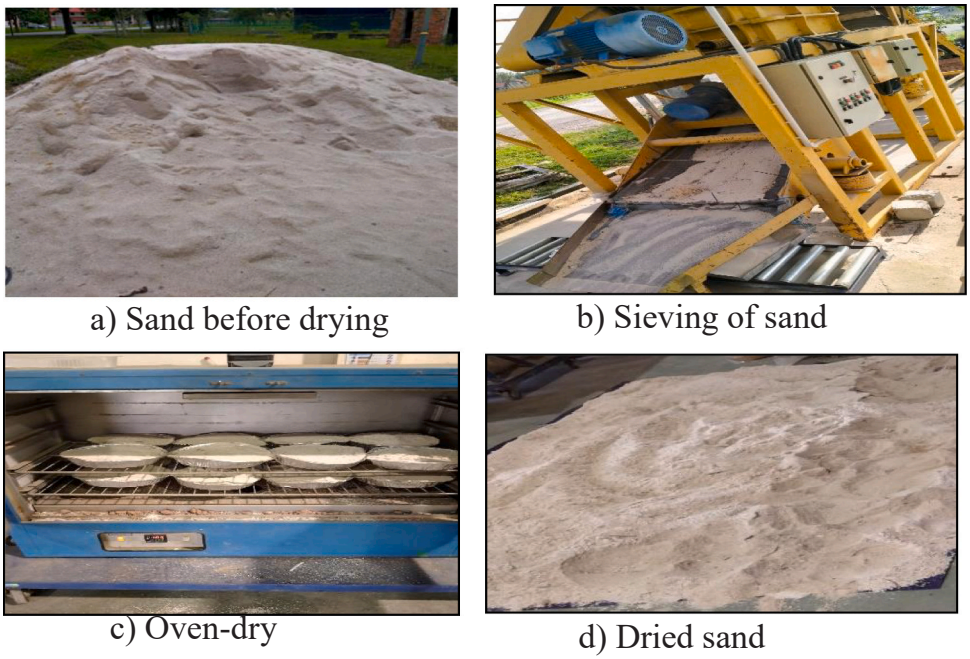

Fig. 2. Process of the preparation of dried sand.

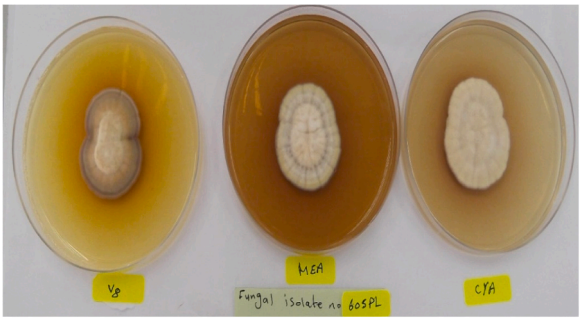

Fig. 3. Pure culture of *Aspergillus iizukae* EAN605 on V8 agar, Malt extract agar (MEA) and Czapek yeast extract agar (CYA).

ensure that the fungi were evenly distributed. In this study, Synthetic foaming agent was used to produce air bubbles in foamed concrete mixture with and without fungi.Various percentages of foam were incorporated into the mixes to achieve the desired densities, and the results are presented in (kg/m^3) per cubic meter of the dried weight. The foaming agent was mixed with water in a ratio of 1:20 and aerated to reach a density of 65 kg/m^3, as per ASTM C796 standards [86,87].

2.2. Methods

2.2.1. Preparation of A. iizukae EAN605

The fungal strain was obtained from peat soil in Kampung Medan Sari (1°28'24.5"N 103°26'35.96"E) in Pontian, Johor, Malaysia, as described by Noman [88]. The fungal strain was described on Malt Extract Agar (MEA) Medium, V8 and Czapek yeast extract agar CYA medium (Fig. 3). *Aspergillus iizukae* EAN605 was prepared by culturing one litre of sterilised pumpkin medium broth (EVA medium) for 3 days at 28 °C, and 150 rpm at high production of fungal biomass was obtained. Fungal biomass was separated by centrifugation at 13,000 rpm for 10 min at 4 °C, washed twice with 10 ml of sterile sodium acetate buffer (pH=5) to remove any remaining medium before being re-suspended in the same buffer. The fungal concentrations in the suspension were estimated as colony-forming units using the direct plate technique on the PDA medium, according to Noman [89]. *Aspergillus iizukae* EAN605 was added to the concrete mixture with different concentrations (0.1, 0.3, 0.5, and 0.64 g/L) to optimise the compressive strength of B-FC using RSM methods. The incorporation of fungi in the concrete mixture was prompted by its isolation from soil, a fundamental constituent that forms an essential part of the concrete matrix. As a consequence, this particular strain of fungus showcases a remarkable capacity to adapt and flourish amidst the inhospitable conditions prevalent within concrete structures, including the formidable challenge posed by an alkaline pH level exceeding 12. Hence, this specific fungus exhibits an impressive aptitude for adjusting and thriving within the demanding environment of concrete, making it an ideal candidate for incorporation into concrete structures.

2.2.2. Design of experiment using RSM

In RSM, a central composite design (CCD) was employed [90]. It involves the use of mathematical and statistical methods to design experiments that can identify the relationships between independent variables (factors) and responses [91]. In other meaning, CCD can optimise the variables to achieve the best possible responses [92]. In this study, a CCD was utilised to investigate three variables at three different levels. Various low and high settings variables were analysed using Minitab software (version 18, Pennsylvania State University, State College, PA, USA). In the design, density was designated as A, *Aspergillus iizukae* EAN605 was designated as B, and the W/C ratio was designated as C. As CCD recommended, the variables were studied at three levels, with two additional levels for each. The aim was to relate the variables more precisely to the response by testing the values lower or higher than the variable levels deduced from the Analysis of Variance (ANOVA) data, as shown in Eq. (1).

In Table 4, an overview of the factors utilized in the study is presented, including their levels of minimum, upper, and middle are presented. This table serves to illustrate the range within which each factor was varied during the experiments.The densities and water-to-cement (w/c) ratio values used in the study were obtained from previous research [93]. while the appropriate proportions of fungi, were determined through a series of trials and mixing experiments. On the other hand, Table 5 showcases the statistical method employed, Response Surface Methodology (RSM), and presents the number of mixtures generated as part of the experimental design. These tables offer valuable insights into the factors considered and the experimental setup undertaken for the study.

ANOVA was carried out to examine any connections between factors and the impact of each factor. A suitable regression model was applied, as shown in Eq. (1) [90,91].

$$Y = B_0 + \sum_i^k B_i \quad X_i \quad + \sum_i^k B_{ii} X2_{ii} + \sum_{ij}^k B_{ij} X_i X_j + E \tag{1}$$

In this equation, Y represents the response, *XiXj* refers to the variables, *k* signifies the number of parameters involved in the experiment, β stands for the regression coefficient, and *e* represents the random error.The metrics that may be used to validate the model's precision and accuracy are the root means square, mean square error, relative per cent deviation, predicted R2, and adjusted R2.

2.2.3. Design of foam concrete mix

The balanced proportions of cement and sand per weight were determined to be 1:1.35, utilising the mix design approach according to ACI 523.3 R [85]. A total of 20 experiments were conducted based on the selected variables as suggested by the CCD using Minitab

Table 4
Variables and levels of variables utilised in response surface methodology (RSM).

Variables	Designated	Variable levels of code		
		Low:− 1	Intermediate: 0	High:+ 1
Density (kg/m^3)	A	1300	1550	1800
A. iizukae EAN605 (*g/l*)	B	0.1	0.3	0.5
W/C ratio	C	0.5	0.55	0.6

Table 5
The experimental runs for the test pieces using RSM.

Run No.	Density (kg/m^3)	Cement (kg/m^3)	Fine sand (kg/m^3)	Water (L/m^3)	W/C ratio	F (g/L)
R1	1300	553.2	746.8	276.6	0.5	0.1
R2	1800	766.0	1034	383	0.5	0.1
R3	1300	553.2	746.8	276.6	0.5	0.5
R4	1800	766.0	1034	383	0.5	0.5
R5	1300	553.2	746.8	276.6	0.6	0.1
R6	1800	766.0	1034	383	0.6	0.1
R7	1300	553.2	746.8	276.6	0.6	0.5
R8	1800	766.0	1034	383	0.6	0.5
R9	1129.55	480.0	674.3	204.1	0.55	0.3
R10	1970.4	838.49	1106	455.4	0.55	0.3
R11	1550	659.5	890.4	329.7	0.55	0.3
R12	1550	659.5	890.4	329.7	0.55	0.6
R13	1550	659.5	890.4	329.7	0.46	0.3
R14	1550	659.5	890.4	329.7	0.63	0.3
R15	1550	659.5	890.4	329.7	0.55	0.3
R16	1550	659.5	890.4	329.7	0.55	0.3
R17	1550	659.5	890.4	329.7	0.55	0.3
R18	1550	659.5	890.4	329.7	0.55	0.3
R19	1550	659.5	890.4	329.7	0.55	0.3
R20	1550	659.5	890.4	329.7	0.55	0.3

18 software. Fourteen experiments were tested with 6 replicates of the average case with compressive strength after 28 days as the response. The replication was performed at the mid-level to increase the precision of the experiment. The experimental design is shown in Table 5. The interaction between the variables (A, B, and C) and the response (compressive strength) was analysed through analysis of variance (ANOVA). To assess the quality of the quadratic prediction models, the model terms, statistical significance of model terms, coefficient of determination (R^2), probability (P-value) with 95 % confidence, and t-test at 5 % significance level (Prob $<$ 0.05) were evaluated.

2.2.4. Specimens' preparation and curing

The FC and B-FC samples were made in a 100 $\times$ 100 $\times$ 100 mm mould. The study followed the guidelines in BS 6073–2:2008, and six samples (3 FC and 3 B-FC) were used for each run. Preparing FC and B-FC samples involved several steps, as illustrated in Fig. 4.

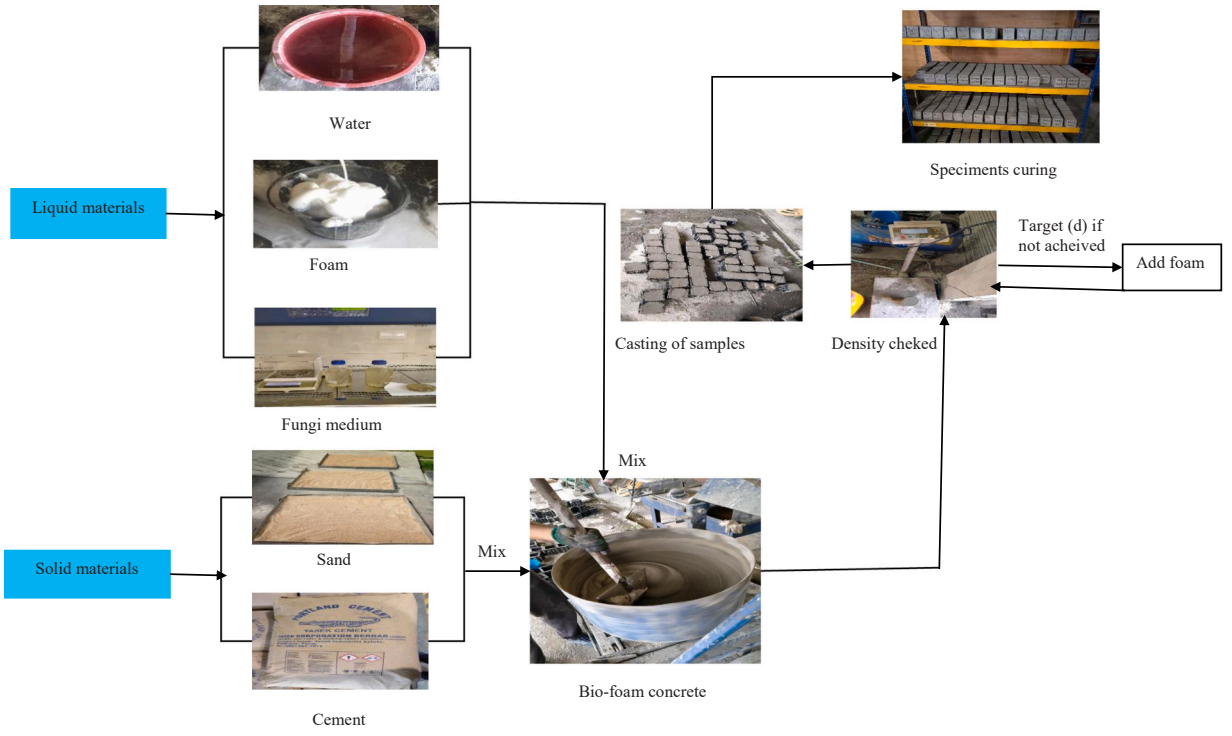

Fig. 4. The curing process of bio-foamed concrete specimens.

First, a foaming agent was mixed with water in a specific ratio, usually around 1:20, and introduced to the foaming equipment. The foam will allow for a uniform paste when mixed with cement, sand, and water. The paste was then placed into moulds and compacted using an external vibrator.

After 24 h, the specimens were removed from the moulds, and the curing process began. Curing is an important step in the preparation of FC and B-FC samples, as it allows the concrete to reach its maximum strength and durability. Curing is typically performed by keeping the cubes in a controlled environment, such as a laboratory storage area, at a specific temperature and humidity range. The temperature is usually between 25 and 32 °C, and the humidity is between 50 % and 74 % RH [18,94].

For B-FC, the addition of microbial additives, *Aspergillus iizukae* EAN605, before the curing process enhances the overall performance and durability of the B-FC without increasing its density. The microbial additives were first mixed with water and thoroughly combined with the paste before compaction. The curing period for FC and B-FC samples was set at 28 days, as suggested by the RSM method (Table 5). This ensures that the specimens can reach maximum strength and durability before testing.

2.2.5. Compressive strength testing

The FC and B-FC compressive strengths were tested to determine their maximum resistance to axial loading. This testing was done by applying compression stress to a 100 × 100 × 100 mm cube-shaped specimen and measuring the highest stress it could withstand. A total of 120 specimens of both FC and B-FC were cast for 20 runs to determine the compressive strength at 28 days. Three samples of each FC and B-FC underwent the compressive strength test to get the average values. The compressive strength was determined by dividing the maximum load applied to the sample by its cross-sectional area, as outlined in BS 1881–116: 1983 [95]. This was done using a machine with a capacity of 1000 kN and a loading rate of 5.0 kN/s, as depicted in Fig. 5. The results of the 20 runs were analysed using a statistical method called RSM to study the effect of various factors on the strength of B-FC. This test was performed on all FC and B-FC, and the results were used to compare and analyse the effects of incorporating *Aspergillus iizukae* EAN605 on the compressive strength of the concrete. Finally, the optimisation of compressive strength for B-FC was analysed using the results from the 20 runs.

2.2.6. Microstructures

X-ray diffraction (XRD) and scanning electron microscopy (SEM) with energy-dispersive X-ray spectroscopy (EDS) are methods that can be used to test the compressive strength of FC and B-FC. XRD is a powerful analytical technique used to determine materials' crystal structure, phase purity, and crystallite size. For XRD, the samples were crushed into a fine powder by drilling, sieved to the size of 300 μm and placed in plates. This process helps to ensure that the samples are homogeneous and that the XRD analysis will yield accurate results.

The SEM is an imaging technique that uses a high-energy electron beam to create a detailed image of the surface of a material. The FC and B-FC SEM samples were small fragments taken from the compressive strength test residue and attached to the mould. The length of the SEM sample was around 2 cm to prevent damage to the specimen, and a very thin layer of carbon was applied to its surface. The samples were then coated using a JFC-1600 auto-fine coater at 20 kV to enhance the conductivity of the specimens and bring their charge closer to neutral. The samples were then scanned using XRD equipment, producing a diffraction pattern unique to each material. The diffraction pattern can then be analysed to determine the crystal structure, phase purity, and crystallite size of the samples. This information is useful in understanding the microstructure of materials and how they may have been affected by the presence of fungi.

The XRD and SEM results were then used to compare the microstructure and composition of the FC and B-FC. The compressive strength of the samples was determined by the load applied to them until they broke and the cross-sectional area of the samples. The compressive strength results were correlated with the XRD and SEM results to understand the relationship among the samples' microstructure, composition, and compressive strength. This can give an insight into how the addition of fungi affects the compressive strength of B-FC and how they compare to the regular FC.

Fig. 5. The compressive strength machine.

3. Results and discussion

3.1. Compressive strength

The compressive strength test results for 20 runs of FC and B-FC using three independent variables, *Aspergillus iizukae* EAN605 concentration, density, and w/c ratio, were analysed and discussed as shown in Fig. 6. The test was conducted on FC and B-FC, and the results were analysed to determine the effect of adding *Aspergillus iizukae* EAN605 on the compressive strength of B-FC. The findings indicated that the addition of *Aspergillus iizukae* EAN605 to the FC mixture resulted in a significant improvement in the compressive strength of the B-FC. Overall, the results indicated that the compressive strength of B-FC was higher than FC in all runs, suggesting that the addition of *Aspergillus iizukae* EAN605 can enhance the properties of B-FC by improving the formation of calcium carbonate.

The finding revealed that runs 2, 4, 6, 8, and 10 demonstrated the highest compressive strength among the 20 runs. Additionally, the compressive strength of B-FC samples was improved by 6.34 %, 37.31 %, 6.61 %, 97 %, and 4.96 %, respectively, compared to that of FC. This was observed at densities of 1800 and 1970 kg/m^3, with fungi levels of 0.1, 0.5, and 0.33 l/g and w/c ratios of 0.5, 0.06, and 0.55. Overall, the results indicate that a high level of *Aspergillus iizukae EAN605* and a decrease in the w/c ratio significantly impact the compressive strength, particularly at high densities. The density of runs 2, 4, 6, and 8 samples is the same at 1800 kg/m^3, but their strengths differ. This suggests that strength can be influenced by more than just density and that the three factors are related to increasing or decreasing strength. For instance, runs 4 and 6 samples have the same density of 1800 kg/m^3, different strengths of 27.5 MPa for run 4 and 13.6 MPa for run 6. The difference in strength can be attributed to the varying ratios and levels of *Aspergillus iizukae* EAN6 in the runs: run 4 has 0.5 of a w/c ratio and 0.5 of *Aspergillus iizukae* EAN605 level, while run 6 has a ratio of 0.6 and a fungi level of 0.1. Additionally, although the compressive strength for run 10 is lower than run 4, run 10 has the highest density (1970 kg/m^3). This difference was because run 4 had a higher proportion of *Aspergillus iizukae* EAN605 (0.5) and a lower w/c ratio (0.5) compared to run 10 (w/c ratio of 0.6 and a lower amount of fungi of 0.1). This result demonstrates that the strength depends on all factors, not just the density. Furthermore, the runs with densities of 1129 kg/m^3, 1300 kg/m^3, and 1550 kg/m^3 produced similar results for B-FC and FC compressive strength. The higher compressive strength of B-FC is likely from the deposition of fungal biominerals in the pores of the cement matrix, effectively blocking the openings within the B-FC. In a case study conducted in Nazareth, Israel, fungal biomineral formation was observed during the creation of calcretes, indicating that fungi can stimulate the formation of biominerals. The formations were identified as calcified filaments [96]. The data were further analysed using XRD and SEM to identify the microstructures of the samples.

3.2. Mathematical modelling and statistical analysis of RSM

The RSM analysis was carried out to optimise the compressive strength of B-FC. This analysis aimed to gain better insight into the effect and correlation between the three selected variables. ANOVA was also used to identify the key variables contributing to the compressive strength and examine the interaction between the input parameters. This was important to obtain more precise results from the data analysis, providing a better understanding of the impact of the selected variables on the compressive strength of the B-FC. The effectiveness of the ANOVA process was studied using the following five major steps: 1) calculating the sum of squares (SS), 2), determining the degrees of freedom (DOF), 3) calculating the mean squares (MS), 4) ceterming the test ratio (F0), and 5) concluding the results.

The ANOVA analysis highlights the significant factors in response, which are presented in a Pareto chart. Furthermore, single factors' performance and interactions were studied to determine their relationship and reflect their effect on the response. The residual plot demonstrated the results' normal distribution. Next, the empirical model equation and optimisation plot were suggested by the ANOVA results. The outcomes of the optimisation procedure for each answer are discussed in depth in the following section.

3.2.1. Analysis of ANOVA for compressive strength for B-FCC

The Analysis of Variance (ANOVA) was conducted to evaluate the compressive strength of bio-foamed concrete cubes B-FC. The purpose of the ANOVA was to determine the most significant factors affecting the compressive strength and to analyse the interactions between the input variables. The results from the ANOVA helped rank the main effects and determine the most important variables

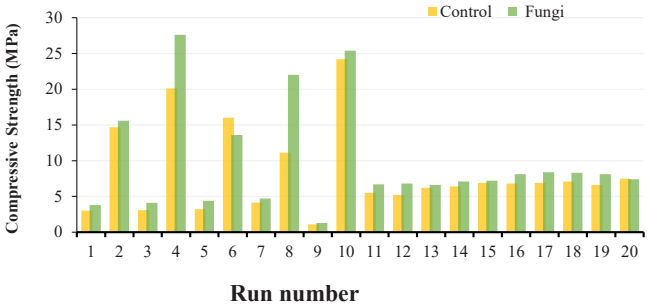

Fig. 6. Compressive strength of FC and B-FC.

that impacted the compressive strength. This information was crucial in optimising the compressive strength and improving the performance of the B-FC.

The ANOVA results for the response surface models are presented in Table 7. These results include information such as the sum of squares, degrees of freedom, mean, F value, and p-value, calculated at a significance level of 0.05. If the p-value exceeds 0.05, the model is considered insignificant. The results from the Table indicate that the model for compressive strength was statistically significant, as evidenced by the high F value (24.80) and low p-value (<0.05). The variables of density (D) and *Aspergillus iizukae* EAN605 (F), as well as their interaction (D*F), all had a significant impact on compressive strength, with p-values of 0.000, 0.016, and 0.010, respectively. Additionally, the results revealed that the square effect of the density (D^2) also significantly impacted the compressive strength. However, in the case of the water-to-cement ratio w/c, although it does have an impact on the strength, the influence is minimal. This is attributed to the narrow range of w/c 0.5–0.6 used, which is close to each other, resulting in a lack of distinct or noticeable effects. Consequently, this observation could serve as a valuable guideline for future research endeavours in this particular field. Further investigations could explore the impact of different water-to-cement ratios on strength properties in order to gain a more comprehensive understanding of their relationship. The improvement in compressive strength was because these factors play a crucial role in determining the strength of B-FC. The density of the material affects its weight and overall strength, while the presence of fungi plays a crucial part in the biomineralisation of calcium carbonate in microbes and is involved in both the biological induction of biomineralisation and organomineralisation processes as described by [55]. Furthermore, fungi boast a significant amount of biomass, and some species grow filaments that can be used as microfibers in materials, resulting in improved strength and reduced porosity [52]. The accuracy of the model was assessed using the coefficient of determination (R^2) and standard deviation (SD) values. The absence of a fit test confirmed that the models were significant. A favourable comparison was found between the predicted R^2 and adjusted R^2 for compressive strength, and the difference between them was less than 20 %, indicating that the model's response was highly accurate [97], as shown in Table 6. In addition, the R^2 value for the compressive strength response was 94.75 %, resulting in a model being considered a good fit if its R^2 value was at least 80 %. An R^2 value close to 100 indicates a strong agreement between the predicted and experimental results [98].

3.2.2. The Pareto chart for standardised compressive strength impacts

The compressive strength results obtained from the Design of Experiments (DOE) are showcased in Table 7, highlighting the determination of variable levels through the proposed model analysis. The statistical significance of the model was confirmed by the calculated p-value being lower than the standard threshold ($p < 0.05$). The statistical significance of the model was confirmed by comparing the calculated p-value with the standard value ($p < 0.05$). This finding aligns with previous literature [99] that established the significance of the model.The Pareto chart demonstrated the standardised impact of compressive strength by analysing three variables: density, *Aspergillus iizukae* EAN605 concentration and w/c ratio. The chart provided valuable insights into the most influential factors that affect the compressive strength of B-FC, and it can be used as a guide for further research and improvement. Notably, the bars in the chart intersect with the reference line at 2.20, indicating the model's noteworthy and statistically significant outcomes. The evaluation of the variables that influence the compressive strength of composite samples was carried out using a factorial model.The results of the variance analysis indicate that the two main variables, density (A) and *Aspergillus iizukae* EAN605 (B), as well as their interaction, have direct effects effect on compressive strength (p-value 0.05) (Fig. 7). However, the w/c only showed minor effects due to the limited range of water-to-cement (w/c) ratios, specifically within the narrow range of 0.5–0.6. The close proximity of these ratios to each other led to a lack of clear or noticeable effects. It was also found that the compressive strength improved with increasing density, reaching up to 1800 kg/m^3. However, based on previous studies, it was decided to keep the density of the foam concrete below 1800 kg/m^3, as densities above this value are used for traditional concrete [100]. Table 8 presents the values of R2, adj. R2, and pred. R2 for the compressive strength analysis. The R2 value of 0.9475 indicated a favorable outcome, as it demonstrated a strong explanation of the relationship between the independent variables and the response. Moreover, the pred. R2 value of 0.9442 showed a reasonable agreement with the adj. R2 value of 0.9093 [101].

3.2.3. Residual plot for compressive strength of B-FC

The residual plot analysis is an important step in understanding the performance of the statistical model. Fig. 8 in this research displays the residual plots for the compressive strength of B-FC using three variables, including density, fungi, and w/c ratio. The residual plots provide information about the goodness of fit of the model. In the normal probability plot, the residuals are plotted against a theoretical normal distribution, and if the residuals are normally distributed, the plot should be a straight line. In this study, the normal probability plot for the residuals was found to be a straight line, indicating that the residuals were normally distributed, as

Table 6
Results of the full design of RSM for compressive strength.

Runs	1	2	3	4	5	6	7	8	9	10
CS	3.8	15.64	4.05	27.5	4.43	14.59	4.72	22.0	1.27	25.43

Note: CS= response of compressive strength (MPa)

Runs	11	12	13	14	15	16	17	18	19	20
CS	6.7	6.79	6.58	7.08	7.19	8.06	8.38	8.27	8.08	8.5

Note: CS= response of compressive strength (MPa)

Table 7
ANOVA results of compressive strength response surface quadratic model.

Source	Degrees of freedom (DF)	Sum of squares (Adj SS)	Mean square (Adj MS)	F-Value	P-Value
Model	8	957.25	119.657	24.80	0.000
Linear	3	803.10	267.699	55.48	0.000
D	1	762.12	762.122	157.95	0.000
F	1	38.99	38.992	8.08	0.016
W/C	1	1.98	1.982	0.41	0.535
Square	2	97.01	48.503	10.05	0.003
D*D	1	95.74	95.740	19.84	0.001
F*F	1	0.04	0.040	0.01	0.929
2-Way Interaction	3	57.15	19.050	3.95	0.039
D*F	1	46.95	46.948	9.73	0.010
D* W/C	1	9.03	9.031	1.87	0.199
F* W/C	1	1.17	1.170	0.24	0.632
Error	11	53.08	4.825		
Lack-of-Fit	6	51.85	8.642	35.3	0.001
Pure Error	5	1.22	0.245		
Total	19	1010.33			

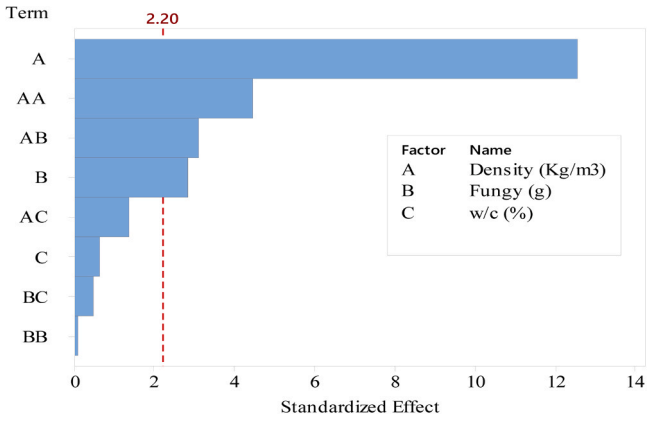

Fig. 7. Pareto chart of compressive strength.

Table 8
Model summary statistics.

Response	Stander deviation	R^2 (%)	Adjusted R^2 (%)	Predicted R^2 (%)	Difference between adjusted R^2 and predicted R^2 (%)	*p*-value
CS,28 day	2.19663	94.75 %	90.93 %	94.42 %	3.67	0.000

confirmed by the symmetry of the residual histogram. The residual versus fit plot and the residual versus plots show that the residuals are independently distributed, as they are randomly scattered on either side of 0, without any clear pattern. The plots also indicate that the model fits the data well. When a statistical model is used to describe a set of data, the residuals are the differences between the observed data points and the values predicted by the model. The residuals should be randomly scattered on either side of 0 if the model fits the data well because this means that the model is not systematically overestimating or underestimating the data.

Both residual versus fit and residual versus order plots are useful for checking the statistical model's assumptions and diagnosing problems with the model fit. The straightness of the normal probability plot and the random distribution of residuals suggests that the statistical model used to analyse the compressive strength of B-FC is appropriate, and the results are trustworthy. However, if the residuals are not randomly scattered on either side of 0, it suggests an issue with the model and further investigation is needed.

3.2.4. Interaction plot for compressive strength of bio-foamed concrete B- FC

The results of the interaction plot for the compressive strength of bio-foamed concrete B-FC are shown in Fig. 9. This plot provides insight into the relationship between the three primary factors of density (kg/m^3), *A. iizukae* EAN605 (g/L), and w/c ratio and their impact on the compressive strength of B-FC. It can be observed from the plot that the interaction between the three factors has a significant impact on the compressive strength of B-FC. According to the graph, the compressive strength of B-FC increases with increasing density and A. iizukae EAN605 while decreasing with increasing w/c ratio. This observation highlights the importance of

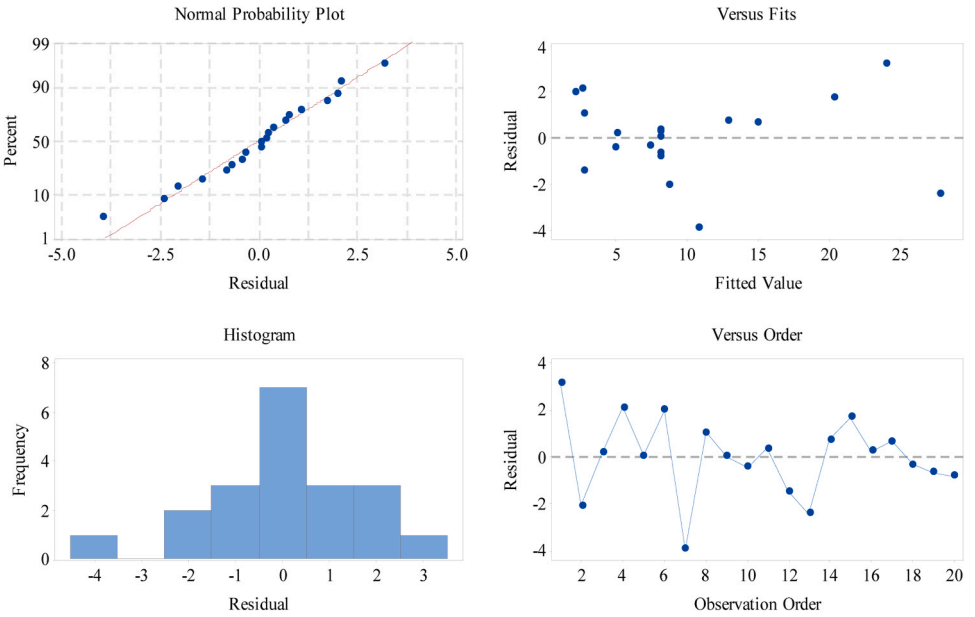

Fig. 8. The compressive strength of B-FC, as shown by the residual plot.

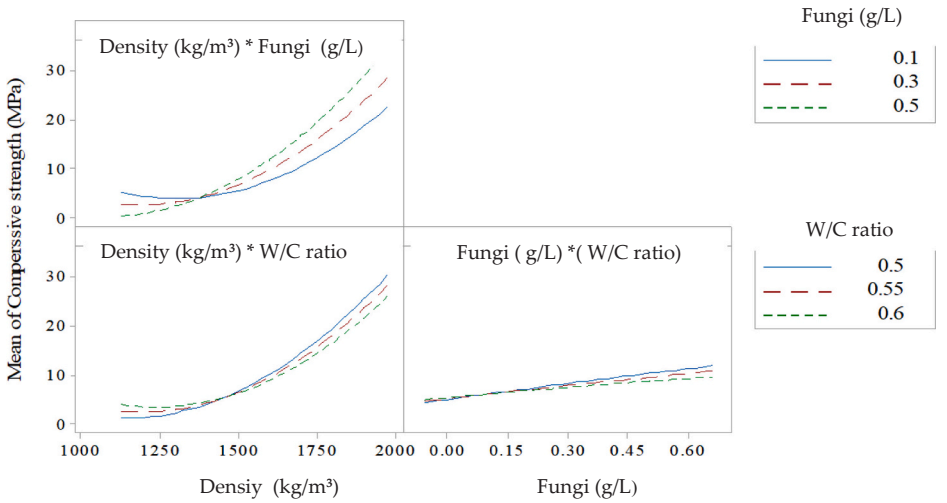

Fig. 9. Interaction plot for compressive strength of bio-foamed concrete B- FC.

Table 9
The ranking for coefficient values of significant factors in the compressive strength of bio-foamed concrete B-FC.

Factor	Effects	Ranking
Density	7.474	1
Fungi	1.682	4
w/c ratio	−0.389	6
Density*Density	2.570	2
Fungi*Fungi	−0.052	8
Density *Fungi	2.423	3
Density * w/c ratio	−1.062	5
Fungi *w/c ratio	−0.382	

balancing these three factors to achieve optimal compressive strength performance in B-FC. The results of the interaction plot revealed that the highest interaction was between density and *A. iizukae* EAN605, with an effect value of 2.423, as shown in Table 9. The strength of concrete was assessed based on the P-values presented in Table 7, determining the influence of each factor. A lower P-value indicates a stronger impact on the strength of the concrete, highlighting the significance of that particular factor.This highlights a strong correlation between the density and *A. iizukae* EAN605 parameters, leading to the accumulation of $CaCO_3$ and high compressive strength for the B-FC. On the other hand, the lower interactions were between *A. iizukae* EAN605 and the w/c ratio, with effect values of 0.382. The *A. iizukae* EAN605 *w/c ratio interaction can be interpreted as follows: the interaction between *A. iizukae* EAN605 *w/c may not be as directly relevant to compressive strength, as fungi primarily affect the durability and long-term performance of concrete, rather than its strength.

On the other hand, bio-foamed concrete has a higher porosity and lower density than normal concrete, making it more susceptible to water uptake and biogenic degradation by fungi, leading to an increase in the w/c ratio and a reduction in the compressive strength of the concrete. The ANOVA results also confirmed that all variables and interactions significantly impacted the compressive strength of B-FC, except for the interaction between *A. iizukae* EAN605 and w/c ratio, which appeared to have a limited effect.

3.2.5. Response surface and contour plots for compressive strength of bio-foamed concrete B- FC

. Fig. 10 illustrates the response surface and contour plots for the compressive strength of B-FC and represent the relationship between the various of density, fungi, and w/c ratio and their impacts on compressive strengt. The purpose of the two plots, a contour plot and a 3D response surface plot, is to analyse and understand how changes in the variables affect the compressive strength of the B-FC. The contour plot provides a 2D representation of the relationship between the variables, while the 3D response surface plot provides a visual representation that includes the third variable as contour lines. These plots demonstrate the interaction between density and fungi (Figs. 10a and 10b) and the relationship between the w/c ratio and fung (Figs. 10c and 11d) in relation to the enhancement of compressive strength at 28 days. The 3D response surface plot was plotted using the predictive equations obtained from regression analysis, where the variables were plotted on the X and Y axes and the response on the Z-axis [102,103].

The results in Fig. 10(a) and 10(b), start from 0 MPa and range from 10 to 30 MPa and above. In Fig. 11c and 11(d), the results begin at 6 MPa and are described using steps ranging from 1.5 to 12 MPa and more. The contour graphs plotted by the colour-ranging layers show the compressive strength range in the different regions of density, fungi, and w/c ratio. At each point on the graph, the values of density, fungi, and w/c ratio are constantly changing. Using the compressive strength table displayed in Fig. 12b and 12(d), it is easy to determine the compressive strength [104]. The relationship between the density, fungi, and w/c ratio and their effect on the

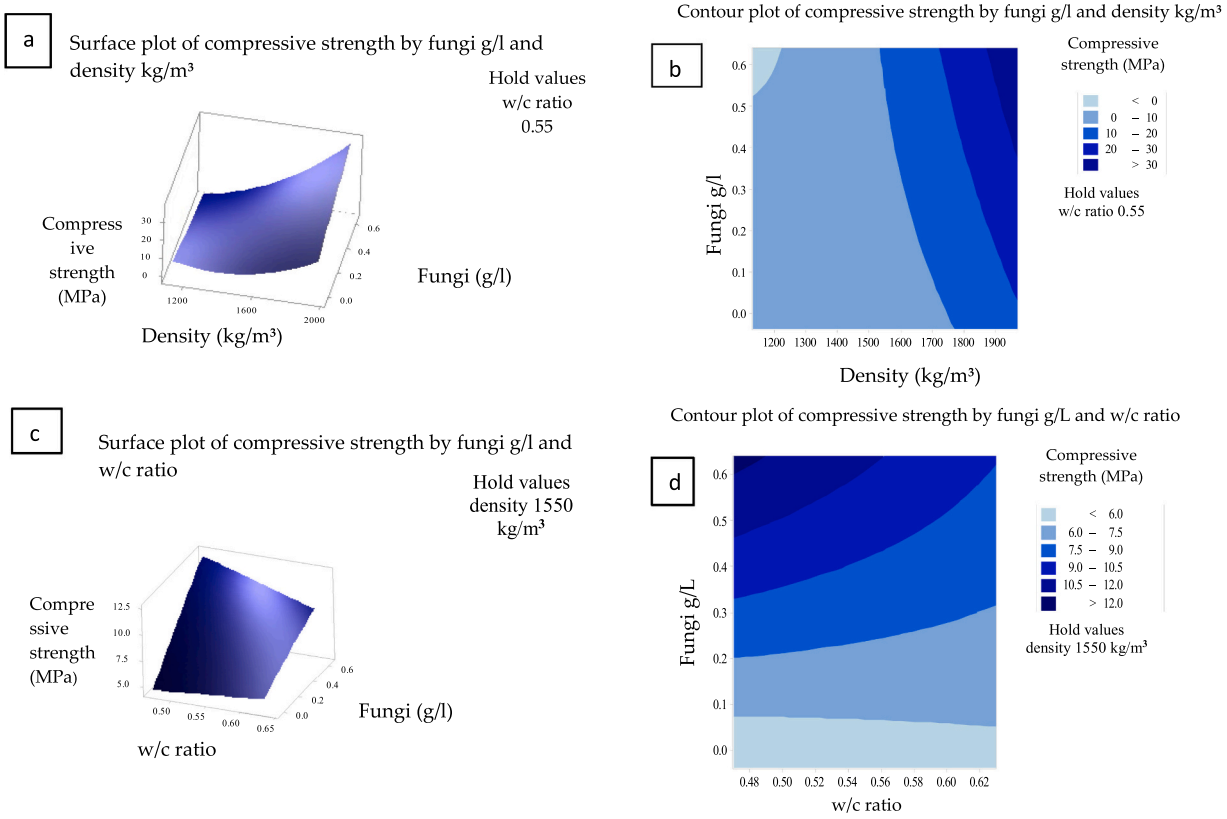

Fig. 10. Response surface and contour plots for compressive strength of B-FC.

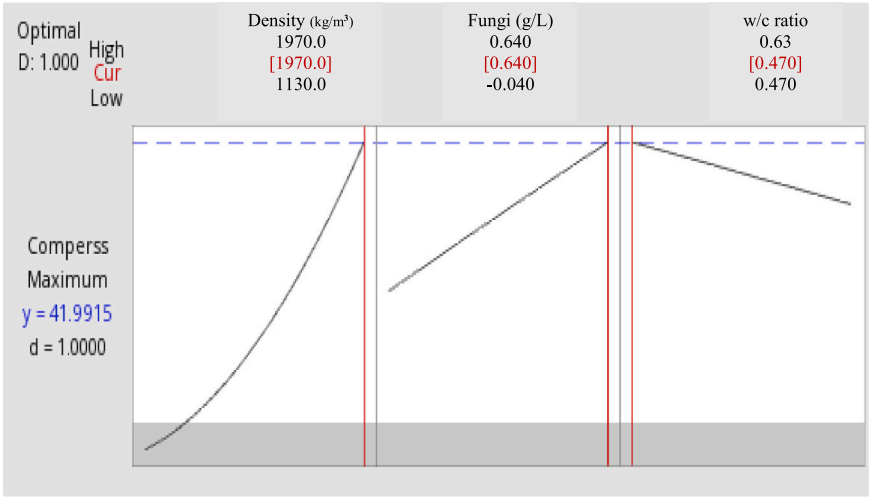

Fig. 11. Response optimisation plots for compressive strength of B-FC.

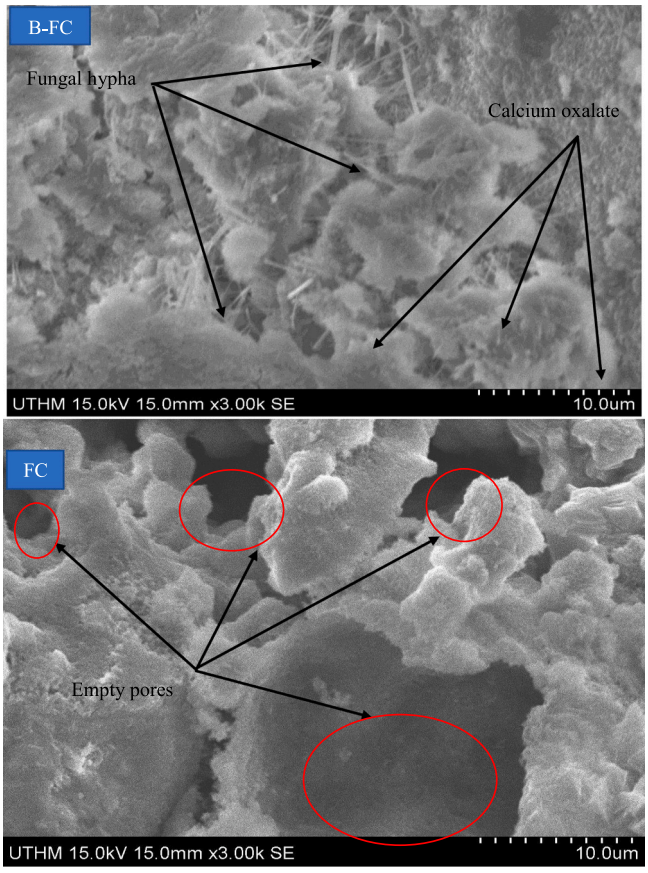

Fig. 12. SEM pictures showing the surfaces of FC (control); calcium oxalate generated by *A. iizukae* EAN 605 at 28 days.

compressive strength can be seen through the contour plot and 3D response surface plot in Fig. 10.

Fig. 10a and b depict the relationship between density and fungi and their effect on the compressive strength of B-FC. The results showed that the compressive strength increased with an increase in density and fungi content, with a maximum strength of over 30 MPa achieved at a density above 1900 kg/m^3 and a fungi content of 0.4–0.6 g/L. In contrast, the minimum value of 10 MPa of compressive strength was recorded at a fungi range of 0–0.5 g/L and a density range of 1200–1800 kg/m^3. Therefore, it can be

concluded that fungi and density play a crucial role in determining the compressive strength of bio-foamed concrete B-FC if they are balanced to ensure the optimal compressive strength of the material. Meanwhile, Figs. 10c and 10(d) show that a w/c ratio of 0.48–0.56 and fungi content of 0.6 g/L resulted in the highest compressive strength of more than 12 MPa. However, the lowest compressive strength value was seen at a fungi range of 0–0.1 g/L and a w/c ratio of 0.48–0.68. Overall, the optimum values for each variable that result in the highest compressive strength have been highlighted. Additionally, a lower w/c ratio results in a denser material and increased strength due to less water in the mixture. These findings suggest that the presence of fungi inside the bio-foamed concrete will improve its strength as it stimulates the precipitation of calcium carbonate in the presence of a nutrient medium [105]. This formation of calcium carbonate will plug the pores between the soil particles, making the soil more firmly bound.

3.2.6. Optimisation plots for compressive strength of B-FC

The optimisation of the compressive strength of bio-foamed concrete B-FC after 28 days was generated using three key variables: fungi, density, and w/c ratio, as shown in Fig. 11**.** The graph showed the relationships between these variables and the resulting compressive strength of the B-FC**.** The 'y' and 'd' values plotted in Fig. 11 denote the maximum strength and desirability value of the process variables, which range from 0 to 1, with "1" indicating the desired combination or ideal and "0" indicating that it is not desirable [97]. The values of each factor that resulted in the greatest possible compressive strength were represented by the solid red lines in the graph. In the meantime, the projected compressive strength is represented by the blue lines with dots. The findings from the study, as depicted in the figure, indicate that the optimal values of density, *A. iizukae* EAN605 and w/c ratio for maximum compressive strength of 41.99 are 1970 kg/m^3, 0.64 g/L, and 0.47, respectively. This suggests that a rise in density, *A. Iizukae* EAN605, and a reduction in the w/c ratio during the curing process result in a higher compressive strength of B-FC. The predictions made in this study regarding the values of density, *A. iizukae* EAN 605, and w/c ratio were in line with the conclusions of previous research. An earlier investigation found that higher levels of density and foam (F) increased compressive strength [106],[105], while an increase in the w/c ratio led to a decrease in compressive strength [107]. After optimising the compressive strength of B-FC using RSM analysis, a predictive model was established to describe the results. The final equation for regression, presented in uncoded units of compressive strength, is given by Equation (2).

Compressive strength (MPa)=5·9–0·0654 density (kg/m^3) - 44·9 fungi (g/L) + 135·5 (w/c ratio) + 0·000041 density (kg/m^3)*density (kg/m^3) - 1·3 fungi (g/L)*fungi (g/L) + 0·0485 density (kg/m^3)*fungi (g/L) - 0·0850 density (kg/m^3)*(w/c ratio) - 38·2 fungi (g/L)*(w/c ratio)

3.2.7. Validation test

The validation of the compressive test was an essential step to ensure the accuracy and reliability of the results obtained. Based on the RSM,the experiment utilised optimal values for density (1970), fungi content (0.64), and water-to-cement (w/c) ratio (0.047). Based on the confirmation, Prior to the validation process, the initial measurement of the compressive strength yielded a value of 41.5 MPa. However, after undergoing validation, the revised compressive strength value was determined to be 39.5 MPa. This validation procedure played a crucial role in verifying the consistency and integrity of the experimental data. The calculated errors between the experimental and optimum results were in the range of + −2 %.

3.3. Microstructure analysis

Microstructure analysis tests play a crucial role in characterising the internal structure of FC and B-FC. SEM and XRD were utilised to analyse the microstructure to examine the healing of pores in the specimens and compare the precipitation of $CaCO_3$ in B-FC and FC.

3.3.1. Scanning electron microscopes (SEM)

The SEM images have shown the surface views of FC and B-FC and variations in the surface morphology of B-FC after the presence of *A. iizukae* EAN605. SEM images revealed that the fungal activity resulted in the creation of calcified filaments and biominerals. These newly formed biominerals filled the pores of B-FC, ultimately reducing its porosity and water absorption due to the biomineral's ability to function as a filler material. The evidence suggests that the hyphae of the fungal species acted as nucleation sites during the mineral precipitation process. These calcified mineral filaments were absent in the FC, as shown in Fig. 12. A previous study [108] also found that fungi can stimulate bio-cement production between grains, which bridges the meniscus and is made up of biomineralised fungal hyphae. The accumulation of ca-oxalates around the fungal spores resulted from the growth of prismatic bipyramidal single crystals, providing further evidence that the crystals form inside a fungal sheath. During the interaction, ca-oxalates formed mostly through encrustation on fungal hyphae. Previous research has linked ca-oxalates to hyphae in various contexts. For example, Kolo [109] suggested that ca-oxalate precipitation on the surfaces of fungal hyphae could serve as a defence mechanism against dehydration and grazing. The crystals strongly adhere to the fungus's hyphae, enabling them to withstand even the mechanical force used in the extraction process.

However, the samples of FC shown in Fig. 12, which were not subjected to fungal treatment, appear to have hollow pores. This absence of treatment leads to decreased compressive strength and increased porosity [44]. Furthermore, the FC samples show trace $CaCO_3$ formation due to the natural carbonation reaction between CO_2 (C-S–H) and $Ca(OH)_2$. The concrete became less solid and more porous. The findings provided evidence that fungi have the potential to enhance concrete strength rather than weaken it. The evidence supporting this lies in the higher strength results compared to the FC. This suggests that the improved compressive strength of B-FC was

due to the fungal biomineral formation that formed on the pores' surfaces, which effectively closed the pores within the concrete. As a result, the permeability of harmful gases like carbon dioxide and water is significantly reduced.

3.3.2. X-ray diffraction (XRD)

The XRD analysis of FCC and B-FC was conducted after 28 days with different densities of 1129, 1300, 1550, 1800, and 1970 kg/m^3, as demonstrated in Fig. 13. The results from XRD analysis of FC and B-FC show the extra peaks of quartz (SiO_2), calcite ($CaCO_3$), calcium hydroxide $(CaOH)_2$, and calcium silicate (Ca_3SiO_5).

Overall, as can be seen from the graphs, the intensity has increased with an increase in density in both FC and B-FC. As a consequence of the reaction of the foaming agent at low densities, numerous large air bubbles are produced compared to high densities. These air bubbles push aside the essential components of cement and calcium, which are required for the synthesis of $CaCO_3$. On the other hand, the results show that the peak intensity in B-FC is significantly lower than in FC, which could indicate less $CaCO_3$ in bio-foamed concrete. Because fungi produce more biomass and some species produce filaments that can act as microfibers in materials, they have proven more effective for biocementation. This could be attributed to fungi that interact with the compounds inside the B-FC physically, leading to the closure of the pores and preventing the entry of carbon dioxide, which interacts with the calcium materials in the concrete. This reduces the formation of calcium carbonate and thus leads to a decrease in the peak intensity of the B-FC. The FC specimens were highly crystalline phases of quartz compared to B-FC samples, as reported by Luo [47]. From this finding, the carbonation process of calcium hydroxide $(CaOH)_2$ occurred in the FC specimens only, based on the following reaction:

$$CO_2 + Ca(OH)_2 \Rightarrow CaCO_3 + H_2O$$

The carbonation results from the dissolution of CO_2 in the concrete pore fluid and its reaction with $Ca(OH)_2$. Figs. 13(j) and 13(h) demonstrate that the greatest intensity of the FC samples was observed at a density of 1800 kg/m^3, with a value of 14000, while for B-FC samples at a similar density, the highest intensity was 11,000, which was higher than the intensity of the samples at other densities. However, at a density of approximately 1129 kg/m^3, both FC and B-FC specimens had lower intensities, with values of approximately 1800 and 1400, respectively. Furthermore, certain peaks were only observed in B-FC samples and were not present in FC samples. For instance, the peaks of calcium silicate hydrate were only visible in B-FC samples and not in FC samples. An XRD investigation confirmed the formation of new silicate phases in B-FC samples, related to an improvement in the concrete's strength.

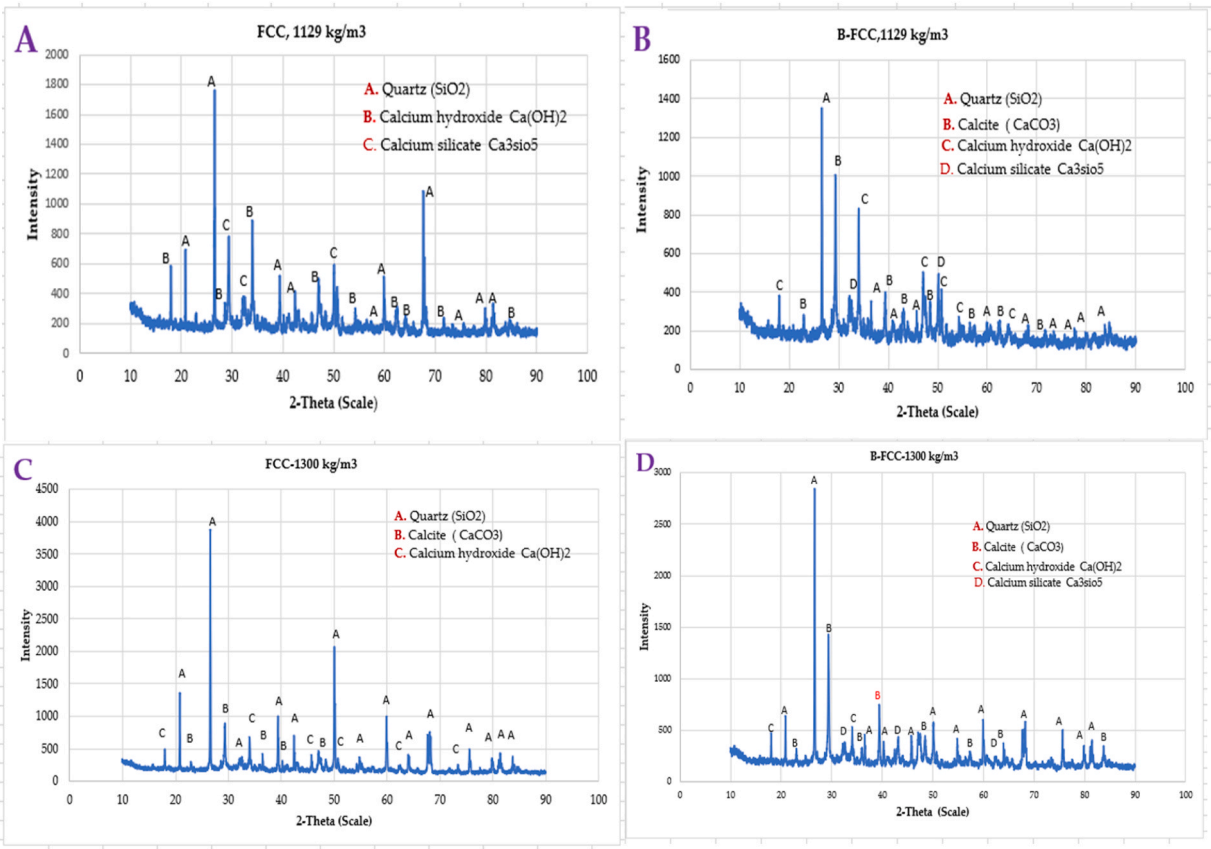

Fig. 13. XRD examination showing a comparison between FC and B-FC at 28-day.

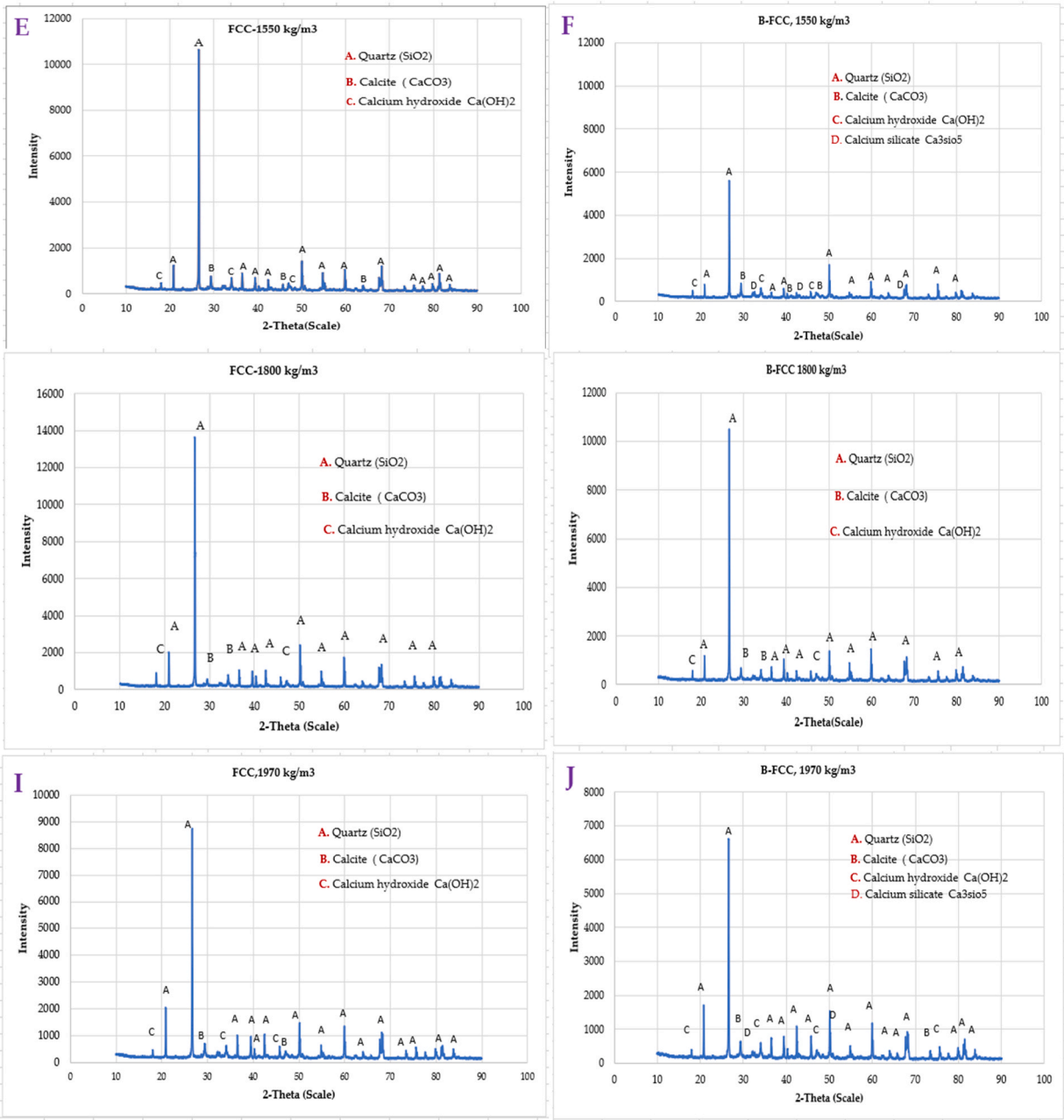

Fig. 13. (*continued*).

4. Conclusion

This work was mainly focused to improve the compressive strength of bio-foamed concrete (B-FC) by incorporating *Aspergillus iizukae* EAN605 as a new type of fungus. Integrating this fungus has proved to be effective in increasing the compressive strength of B-FC, making it a more reliable and durable building material. The use of *Aspergillus iizukae* EAN605 as a biological agent in foam concrete (FC) can provide improved strength and other benefits, such as enhanced durability and resistance to environmental factors and reduced carbon footprint. However, the main conclusions were highlighted in points as follows;.

a. The compressive strength gain of B-FC were between 4.3 % and 97.66 % compared to FC at the curing age of 28 days. The results showed that increasing the compressive strength of B-FC has several possible explanations.

b. One theory is that the fungus generates enzymes that break down the components of the foam concrete, leading to the formation of stronger bonds among the particles. Another possibility is that the fungus generates extracellular polymeric substances (EPS) that act as a binder, enhancing the cohesion of the material and improving its strength.
c. It is also feasible that the fungi triggered the formation of $CaCO_3$, leading to sand biocementation. In other words, the fungi may have caused the precipitation of $CaCO_3$ and facilitated the binding of sand particles through biological processes. The most likely reason for the enhancement in the B-FC's compressive strength is likely a result of the fungal biomineral being deposited inside the pores of the cement matrix. This biomineral fills the gaps in the concrete and prevents further pore formation.
d. The results from the RSM showed that density (D), A. iizukae EAN605 F, and the (w/c ratio) significantly impact achieving the optimal compressive strength of B-FC. The highest compressive strength of B-FC was achieved at a density of 1800 kg/m^3, *A.iizukae* EAN605 of 0.5 g/L, and a w/c ratio of 0.5 which led to a maximum compressive strength of 27.5 MPa.
e. It is from RSM suggested that under certain conditions, such as a density of 1970 kg/m^3, *A. iizukae* EAN605 of 0.64 g/L, and a w/c ratio of 0.47, optimisation would result in improved strength of B-FC and reach a maximum compressive strength of 41.99 MPa. The statistical analysis of the models produced a desirable R^2 value of 94.75 %.
f. Notably, the application of fungi in construction materials is a novel field, and further exploration is required to grasp the mechanisms that lead to increased compressive strength. Despite this, the early outcomes are positive, and the implementation of *Aspergillus iizukae* EAN605 in FC holds the promise of delivering substantial benefits to the construction industry.

Based on the main findings of this study, further investigations are needed to 1) evaluate the durability and long-term performance of FC incorporating fungi; 2) it is also important to keep in mind that the results of this study only apply to the specific type of fungus *Aspergillus iizukae* EAN605 and the specific type of used FC; 3) to replicate the study using different types of fungi and FC to generalise the results; 4) further studies to fully understand the mechanism behind this improvement and to optimise the use of *Aspergillus iizukae* EAN605 in FC.

Declaration of Competing Interest

The authors of this manuscript hereby declare that have no known competing interests or personal relationships that may have influenced the research, or the results presented in this paper. They have confirmed that the research conducted in this paper was done with integrity and without any bias.

Data availability

No data was used for the research described in the article.

Acknowledgments

This study was made possible through a grant from the Ministry of Higher Education Malaysia (MOHE) under the Fundamental Research Grant Scheme (FRGS/1/2019/WAB05/UTHM/02/1), which was supported by Universiti Tun Hussien Onn Malaysia (UTHM) under MDR (VOT no. H486 and H487). Also, this study is supported via funding from Prince Sattam bin Abdulaziz University project number (PSAU/2023/R/1444).

References

[1] I.M. Maafa, A. Abutaleb, N. Zouli, A.M. Zeyad, A. Yousef, M.M. Ahmed, Effect of agricultural biomass wastes on thermal insulation and self-cleaning of fired bricks, J. Mater. Res. Technol. 24 (2023) 4060–4073, https://doi.org/10.1016/j.jmrt.2023.03.189.
[2] E. Namsone, G. Šahmenko, A. Korjakins, Durability properties of high performance foamed concrete, Procedia Eng. 172 (2017) 760–767, https://doi.org/10.1016/j.proeng.2017.02.120.
[3] A. Othuman, Y.C. Wang, Elevated-temperature thermal properties of lightweight foamed concrete, Constr. Build. Mater. 25 (2011) 705–716, https://doi.org/10.1016/j.conbuildmat.2010.07.016.
[4] N.M. Zahari, I.A. Rahman, A. Mujahid, A. Zaidi. Foamed Concrete: Potential Application in Thermal Insulation Heat in Heat out Air- voids Foam Concrete, 2009, pp. 47–52.
[5] S.K. Lim, C.S. Tan, O.Y. Lim, Y.L. Lee, Fresh and hardened properties of lightweight foamed concrete with palm oil fuel ash as filler, Constr. Build. Mater. 46 (2013) 39–47, https://doi.org/10.1016/j.conbuildmat.2013.04.015.
[6] Y.H.M. Amran, N. Farzadnia, A.A.A. Ali, Properties and applications of foamed concrete; a review, Constr. Build. Mater. (2015), https://doi.org/10.1016/j.conbuildmat.2015.10.112.
[7] B. Kado, S. Mohammad, Y.H. Lee, P.N. Shek, M.A. Ab Kadir, Experimental study on behavior of unprotected foamed concrete filled steel hollow column under fire, J. Civ. Eng. Sci. Technol. 12 (2021) 189–202, https://doi.org/10.33736/jcest.3983.2021.
[8] E.P. Kearsley, P.J. Wainwright, The effect of porosity on the strength of foamed concrete, Cem. Concr. Res. 32 (2002) 233–239, https://doi.org/10.1016/S0008-8846(01)00665-2.
[9] E.P. Kearsley, P.J. Wainwright, Porosity and permeability of foamed concrete, Cem. Concr. Res. 31 (2001) 805–812, https://doi.org/10.1016/S0008-8846(01)00490-2.
[10] Y.H.M. Amran, N. Farzadnia, A.A.A. Ali, Properties and applications of foamed concrete; a review, Constr. Build. Mater. 101 (2015) 990–1005, https://doi.org/10.1016/j.conbuildmat.2015.10.112.
[11] M. Amran, R. Fediuk, N. Vatin, Y.H. Lee, G. Murali, T. Ozbakkaloglu, S. Klyuev, H. Alabduljabber, Fibre-reinforced foamed concretes: a review, Materials (Basel) 13 (2020) 1–36, https://doi.org/10.3390/ma13194323.
[12] Y.H. Mugahed Amran, A.A. Abang Ali, R.S.M. Rashid, F. Hejazi, N.A. Safiee, Structural behavior of axially loaded precast foamed concrete sandwich panels, Constr. Build. Mater. 107 (2016) 307–320, https://doi.org/10.1016/j.conbuildmat.2016.01.020.

[13] Y.H.M. Amran, R.S.M. Rashid, F. Hejazi, N.A. Safiee, A.A.A. Ali, Response of precast foamed concrete sandwich panels to flexural loading, J. Build. Eng. 7 (2016) 143–158, https://doi.org/10.1016/j.jobe.2016.06.006.
[14] V. Lesovik, V. Voronov, E. Glagolev, R. Fediuk, A. Alaskhanov, Y.H.M. Amran, G. Murali, A. Baranov, Improving the behaviors of foam concrete through the use of composite binder, J. Build. Eng. 31 (2020), https://doi.org/10.1016/j.jobe.2020.101414.
[15] S.S. Suhaili, N.N. Alias, M.A. Othuman Mydin, H. Awang, Influence of oil palm spikelets fibre on mechanical properties of lightweight foamed concrete, J. Civ. Eng. Sci. Technol. 12 (2021) 160–167, https://doi.org/10.33736/jcest.3980.2021.
[16] Y.H. Mugahed Amran, R. Alyousef, H. Alabduljabbar, M.H.R. Khudhair, F. Hejazi, A. Alaskar, F. Alrshoudi, A. Siddika, Performance properties of structural fibred-foamed concrete, Results Eng. 5 (2020), https://doi.org/10.1016/j.rineng.2019.100092.
[17] Y.H. Mugahed Amran, R.S.M. Rashid, F. Hejazi, A.A. Abang Ali, N.A. Safiee, S.M. Bida, Structural performance of precast foamed concrete sandwich panel subjected to axial load, KSCE J. Civ. Eng. 22 (2018) 1179–1192, https://doi.org/10.1007/s12205-017-1711-6.
[18] S. Saheed, Y.H.M. Amran, M. El-Zeadani, F.N.A. Aziz, R. Fediuk, R. Alyousef, H. Alabduljabbar, Structural behavior of out-of-plane loaded precast lightweight EPS-foam concrete C-shaped slabs, J. Build. Eng. 33 (2021), https://doi.org/10.1016/j.jobe.2020.101597.
[19] P. Shawnim, F. Mohammad, P, P M. F. C. Sem. 10 (2019) 22–33.
[20] M. Amran, Y.H. Lee, N. Vatin, R. Fediuk, S. Poi-Ngian, Y.Y. Lee, G. Murali, Design efficiency, characteristics, and utilization of reinforced foamed concrete: a review, Crystals (2020), https://doi.org/10.3390/cryst10100948.
[21] A.A. Amran, Y.M. Rashid, R.S. Hejazi, F. Safiee, N. A, Ali, Structural behavior of laterally loaded precast foamed concrete sandwich panel, Int. J. Civ. Environ. Struct. Constr. Arch. Eng. 10 (2016) 255–263.
[22] M. Visagie, E.P. Kearsley, Properties of foamed concrete as influenced by air-void, Parameters, Concr. Bet. 101 (2002) 9–13.
[23] P.A. Shawnim, F. Mohammad, Compressive strength of foamed concrete in relation to porosity using sem images, J. Civ. Eng. Sci. Technol. 10 (2019) 34–44, https://doi.org/10.33736/jcest.1005.2019.
[24] Y.H. Mugahed Amran, R. Alyousef, H. Alabduljabbar, F. Alrshoudi, R.S.M. Rashid, Influence of slenderness ratio on the structural performance of lightweight foam concrete composite panel, Case Stud. Constr. Mater. 10 (2019), https://doi.org/10.1016/j.cscm.2019.e00226.
[25] Y.H. Mugahed Amran, Determination of Structural Behavior of Precast Foamed Concrete Sandwich Panel, Universiti Putra Malaysia (UPM), 2016.
[26] M. Abdelgader, H.S. Kurpińska, M, Amran, Effect of slag coal ash and foamed glass on the mechanical properties of two-stage concrete, Mater. Today Proc. 1 (2022) 12.
[27] A.A. Amran, Y.M. Rashid, R.S. Hejazi, F. Safiee, N. A, Ali, Structural behavior of precast foamed concrete sandwich panel subjected to vertical in-plane shear loading, J. Civ. Environ. Struct. Constr. Arch. 10 (2016) 699–708.
[28] and, M.A. Miryuk, Olga, Roman Fediuk, Foam glass crystalline granular material from a polymineral raw mix, Crystals 11 (2021) 1447.
[29] S. Saheed, F.N.A.A. Aziz, M. Amran, N. Vatin, R. Fediuk, T. Ozbakkaloglu, G. Murali, M.A. Mosaberpanah, Structural performance of shear loaded precast EPS-foam concrete half-shaped slabs, Sustain 12 (2020) 1–17, https://doi.org/10.3390/su12229679.
[30] M.R. Jones, A. McCarthy, Heat of hydration in foamed concrete: Effect of mix constituents and plastic density, Cem. Concr. Res. (2006), https://doi.org/10.1016/j.cemconres.2006.01.011.
[31] A.A. Sayadi, J.V. Tapia, T.R. Neitzert, G.C. Clifton, Effects of expanded polystyrene (EPS) particles on fire resistance, thermal conductivity and compressive strength of foamed concrete, Constr. Build. Mater. 112 (2016) 716–724, https://doi.org/10.1016/j.conbuildmat.2016.02.218.
[32] A.A. Hilal, N. Howard, A. Robert, On entrained pore size distribution of foamed concrete, Constr. Build. Mater. 75 (2015) 227–233, https://doi.org/10.1016/j.conbuildmat.2014.09.117.
[33] K. Ramamurthy, E.K. Kunhanandan Nambiar, G. Indu Siva Ranjani, A classification of studies on properties of foam concrete, Cem. Concr. Compos. 31 (2009) 388–396, https://doi.org/10.1016/j.cemconcomp.2009.04.006.
[34] R. Kumar, B. Bhattacharjee, Porosity, Pore Size Distribution and In Situ Strength of Concrete Porosity, pore size distribution and in situ strength of concrete, 8846 (2003). ⟨https://doi.org/10.1016/S0008–8846(02)00942–0⟩.
[35] E.K.K. Nambiar, K. Ramamurthy, Air - void characterisation of foam concrete, 37 (2007) 221–230. ⟨https://doi.org/10.1016/j.cemconres.2006.10.009⟩.
[36] E.K. Kunhanandan Nambiar, K. Ramamurthy, Fresh state characteristics of foam concrete, J. Mater. Civ. Eng. 20 (2008) 111–117, https://doi.org/10.1061/(asce)0899-1561(2008)20:2(111).
[37] F. Salmasi, D. Mostofinejad, Investigating the effects of bacterial activity on compressive strength and durability of natural lightweight aggregate concrete reinforced with steel fibers, Constr. Build. Mater. 251 (2020), 119032, https://doi.org/10.1016/j.conbuildmat.2020.119032.
[38] J.D. Pj, S. Kotteeswaran, Study on properties of foam concrete using fibers, Int. J. Res. Rev. 5 (2018) 187–192.
[39] S.K. Lim, Y.L. Lee, M.K. Yew, W.W. Ng, F.W. Lee, K.Z. Kwong, Mechanical Properties of Lightweight Foamed Concrete With Ceramic Tile Wastes as Partial Cement Replacement Material, 8 (2022) 1–12. ⟨https://doi.org/10.3389/fbuil.2022.836362⟩.
[40] B.pasteurii calcite precipitation.pdf, (2001).
[41] S.S. Ramachandran, S.K. Ramakrishnan, V, Bang, Concrete remediation with B. pasteurii.pdf, Acids Mater. J. 98 (2001) 3–9.
[42] J. Dick, W. De Windt, B. De Graef, H. Saveyn, P. Van Der Meeren, N. De Belie, W. Verstraete, Bio-deposition of a calcium carbonate layer on degraded limestone by Bacillus species, Biodegradation 17 (2006) 357–367, https://doi.org/10.1007/s10532-005-9006-x.
[43] W. De Muynck, D. Debrouwer, N. De Belie, W. Verstraete, Bacterial carbonate precipitation improves the durability of cementitious materials, Cem. Concr. Res. 38 (2008) 1005–1014, https://doi.org/10.1016/j.cemconres.2008.03.005.
[44] J. Wang, K. Van Tittelboom, N. De Belie, W. Verstraete, Use of silica gel or polyurethane immobilized bacteria for self-healing concrete, Constr. Build. Mater. 26 (2012) 532–540, https://doi.org/10.1016/j.conbuildmat.2011.06.054.
[45] H.M. Jonkers, A. Thijssen, G. Muyzer, O. Copuroglu, E. Schlangen, Application of bacteria as self-healing agent for the development of sustainable concrete, Ecol. Eng. 36 (2010) 230–235, https://doi.org/10.1016/j.ecoleng.2008.12.036.
[46] J.Y. Wang, H. Soens, W. Verstraete, N. De Belie, Self-healing concrete by use of microencapsulated bacterial spores, Cem. Concr. Res. 56 (2014) 139–152, https://doi.org/10.1016/j.cemconres.2013.11.009.
[47] J. Luo, X. Chen, J. Crump, H. Zhou, D.G. Davies, G. Zhou, N. Zhang, C. Jin, Interactions of fungi with concrete: Significant importance for bio-based self-healing concrete, Constr. Build. Mater. 164 (2018) 275–285, https://doi.org/10.1016/j.conbuildmat.2017.12.233.
[48] T. Amran, M. Onaizi, A.M. Fediuk, R. Vatin, N.I. Muhammad Rashid, R.S. Abdelgader, H, Ozbakkaloglu, Self-healing concrete as a prospective construction material: a review, Materials (Basel) 15 (2022) 3214.
[49] J. Zhao, L. Csetenyi, G.M. Gadd, Fungal-induced CaCO3 and SrCO3 precipitation: a potential strategy for bioprotection of concrete, Sci. Total Environ. 816 (2022), 151501, https://doi.org/10.1016/j.scitotenv.2021.151501.
[50] V. Lesovik, R. Fediuk, M. Amran, N. Vatin, R. Timokhin, Self-healing construction materials: the geomimetic approach, Sustain 13 (2021), https://doi.org/10.3390/su13169033.
[51] S. Bindschedler, G. Cailleau, E. Verrecchia, Role of fungi in the biomineralization of calcite, Minerals 6 (2016), https://doi.org/10.3390/min6020041.
[52] C. Martuscelli, C. Soares, N. Lima, A. Camões, Potential of fungi to produce biosandstone, (2020) 157–162.
[53] G.M. Gadd, Presidential address Geomycology: biogeochemical transformations of rocks, minerals, metals and radionuclides by fungi, bioweathering and bioremediation, 111 (2007) 3–49. ⟨https://doi.org/10.1016/j.mycres.2006.12.001⟩.
[54] G. Michael, Geomicrobiology of the built environment, (2017). ⟨https://doi.org/10.1038/nmicrobiol.2016.275⟩.
[55] Q. Li, L. Csetenyi, G.M. Gadd, Biomineralization of metal carbonates by Neurospora crassa, Environ. Sci. Technol. 48 (2014) 14409–14416, https://doi.org/10.1021/es5042546.
[56] L.S. Wong, A.F.M. Oweida, S.Y. Kong, D.M. Iqbal, P. Regunathan, The surface coating mechanism of polluted concrete by Candida ethanolica induced calcium carbonate mineralization, Constr. Build. Mater. 257 (2020), 119482, https://doi.org/10.1016/j.conbuildmat.2020.119482.
[57] E.A. Noman, A. Al-Gheethi, N.N.N.A. Rahman, H. Nagao, M. Ab. Kadir, Assessment of relevant fungal species in clinical solid wastes, Environ. Sci. Pollut. Res. 23 (2016) 19806–19824, https://doi.org/10.1007/s11356-016-7161-8.

[58] R.R. Menon, J. Luo, X. Chen, H. Zhou, Z. Liu, G. Zhou, N. Zhang, C. Jin, Screening of fungi for potential application of self-healing concrete, Sci. Rep. 9 (1) (2019) 12, https://doi.org/10.1038/s41598-019-39156-8.
[59] G. Kaur, R. Siddique, A. Rajor, Micro-structural and metal leachate analysis of concrete made with fungal treated waste foundry sand, Constr. Build. Mater. 38 (2013) 94–100, https://doi.org/10.1016/j.conbuildmat.2012.07.112.
[60] G. Kaur, R. Siddique, A. Rajor, Influence of fungus on properties of concrete made with waste foundry sand, J. Mater. Civ. Eng. 25 (2013) 484–490, https://doi.org/10.1061/(asce)mt.1943-5533.0000521.
[61] G. Kaur, R. Siddique, A. Rajor, Properties of concrete containing fungal treated waste foundry sand, Constr. Build. Mater. 29 (2012) 82–87, https://doi.org/10.1016/j.conbuildmat.2011.08.091.
[62] ASTM I, Standard Test Method for Foaming Agents for Use in Producing Cellular Concrete, ASTM Int. 3 (1967) 1–5.
[63] A. Raj, D. Sathyan, K.M. Mini, Physical and functional characteristics of foam concrete: a review, Constr. Build. Mater. 221 (2019) 787–799, https://doi.org/10.1016/j.conbuildmat.2019.06.052.
[64] M.R. Jones, A. McCarthy, Utilising unprocessed low-lime coal fly ash in foamed concrete, Fuel 84 (2005) 1398–1409, https://doi.org/10.1016/j.fuel.2004.09.030.
[65] A. Anwar, S. Israr, F. Ashraf, M. Arkam, M. Junaid, A. Usama. Study on Foamed Concrete, 1999, pp. 53–55.
[66] S. Kolias, C. Georgiou, The effect of paste volume and of water content on the strength and water absorption of concrete, Cem. Concr. Compos. 27 (2005) 211–216, https://doi.org/10.1016/j.cemconcomp.2004.02.009.
[67] M.I. Norlia, R.C. Amat, N.L. Rahim, S. Salehuddin, Performance of lightweight foamed concrete with replacement of concrete sludge aggregate as coarse aggregate, Adv. Mater. Res. 689 (2013) 265–268, https://doi.org/10.4028/www.scientific.net/AMR.689.265.
[68] C. Bing, W. Zhen, L. Ning, Experimental research on properties of high-strength foamed concrete, J. Mater. Civ. Eng. 24 (2012) 113–118, https://doi.org/10.1061/(asce)mt.1943-5533.0000353.
[69] A.F. Roslan, H. Awang, M.A.O. Mydin, Effects of various additives on drying shrinkage, compressive and flexural strength of lightweight foamed concrete (LFC), Adv. Mater. Res. 626 (2013) 594–604, https://doi.org/10.4028/www.scientific.net/AMR.626.594.
[70] X. Tan, W. Chen, J. Wang, D. Yang, X. Qi, Y. Ma, X. Wang, S. Ma, C. Li, Influence of high temperature on the residual physical and mechanical properties of foamed concrete, Constr. Build. Mater. 135 (2017) 203–211, https://doi.org/10.1016/j.conbuildmat.2016.12.223.
[71] P. Ghosh, S. Mandal, B.D. Chattopadhyay, S. Pal, Use of microorganism to improve the strength of cement mortar, Cem. Concr. Res. 35 (2005) 1980–1983, https://doi.org/10.1016/j.cemconres.2005.03.005.
[72] P. Jagannathan, K.S. Satya, ScienceDirect Studies on the mechanical properties of bacterial concrete with two bacterial species, Mater. Today Proc. 5 (2018) 8875–8879, https://doi.org/10.1016/j.matpr.2017.12.320.
[73] S.L. Williams, M.J. Kirisits, R.D. Ferron, Influence of concrete-related environmental stressors on biomineralizing bacteria used in self-healing concrete, Constr. Build. Mater. (2016), https://doi.org/10.1016/j.conbuildmat.2016.09.155.
[74] J. Xu, X. Wang, Self-healing of concrete cracks by use of bacteria-containing low alkali cementitious material, Constr. Build. Mater. 167 (2018) 1–14, https://doi.org/10.1016/j.conbuildmat.2018.02.020.
[75] A.U. Charpe, M.V. Latkar, T. Chakrabarti, Microbially assisted cementation – a biotechnological approach to improve mechanical properties of cement, Constr. Build. Mater. 135 (2017) 472–476, https://doi.org/10.1016/j.conbuildmat.2017.01.017.
[76] S. Bhaskar, K.M. Anwar Hossain, M. Lachemi, G. Wolfaardt, M. Otini Kroukamp, Effect of self-healing on strength and durability of zeolite-immobilized bacterial cementitious mortar composites, Cem. Concr. Compos. 82 (2017) 23–33, https://doi.org/10.1016/j.cemconcomp.2017.05.013.
[77] H.K. Kim, S.J. Park, J.I. Han, H.K. Lee, Microbially mediated calcium carbonate precipitation on normal and lightweight concrete, Constr. Build. Mater. 38 (2013) 1073–1082, https://doi.org/10.1016/j.conbuildmat.2012.07.040.
[78] K. Van Tittelboom, N. De Belie, W. De Muynck, W. Verstraete, Cement and concrete research use of bacteria to repair cracks in concrete, Cem. Concr. Res 40 (2010) 157–166.
[79] Y. Zhang, H.X. Guo, X.H. Cheng, C.À. Caco, C.À. Ca, Role of calcium sources in the strength and microstructure of microbial mortar, Constr. Build. Mater. 77 (2015) 160–167, https://doi.org/10.1016/j.conbuildmat.2014.12.040.
[80] R. Andalib, M. Zaimi, A. Majid, M. Warid, M. Ponraj, A. Keyvanfar, J. Mirza, H. Lee, Optimum concentration of Bacillus megaterium for strengthening structural concrete, Constr. Build. Mater. 118 (2016) 180–193, https://doi.org/10.1016/j.conbuildmat.2016.04.142.
[81] S. Choi, K. Wang, Z. Wen, J. Chu, Mortar crack repair using microbial induced calcite precipitation method, Cem. Concr. Compos. (2017), https://doi.org/10.1016/j.cemconcomp.2017.07.013.
[82] H. Thiyagarajan, S.Q.M. Dq, M. Mapa, S. Krishnam, A.R. Murthy, N.R. Iyer, V.C. Li, E. Herbert, H. Thiyagarajan, S. Maheswaran, M. Mapa, S. Krishnamoorthy, Investigation of bacterial activity on compressive strength of cement mortar in different curing media, J. Adv. Concr. Technol. 14 (2016) 125–133, https://doi.org/10.3151/jact.14.125.
[83] Ms 522: Part 1:2003, Ms 522: Part 1:2003, BSI Stand. Publ. (2003).
[84] BS EN 197–1-2000.pdf, (n.d.).
[85] R. Kumar, R. Lakhani, A simple novel mix design method and properties assessment of foamed concretes with limestone slurry waste, Elsevier B.V. (2017), https://doi.org/10.1016/j.jclepro.2017.10.073.
[86] A.F. Alshalif, I. Jm, N. Othman, A. Al-gheethi, A. Hassan, Potential of carbonic anhydrase and urease bacteria for sequestration of CO 2 into aerated concrete 3004 (2018) 1–11, https://doi.org/10.1016/j.conbuildmat.2020.119482.
[87] Ö. Cizer, E. Ruiz-agudo, C. Rodriguez-navarro, Kinetic effect of carbonic anhydrase enzyme on the carbonation reaction of lime mortar, 3058 (2018). ⟨https://doi.org/10.1080/15583058.2017.1413604⟩.
[88] E. Noman, A.A. Al-Gheethi, B.A. Talip, R. Mohamed, A.H. Kassim, Oxidative enzymes from newly local strain Aspergillus iizukae EAN605 using pumpkin peels as a production substrate: Optimized production, characterization, application and techno-economic analysis, J. Hazard. Mater. 386 (2020), 121954, https://doi.org/10.1016/j.jhazmat.2019.121954.
[89] E. Noman, A.A. Al-Gheethi, B. Talip, R. Mohamed, A.H. Kassim, Mycoremediation of Remazol Brilliant Blue R in greywater by a novel local strain of Aspergillus iizukae 605EAN: optimisation and mechanism study, Int. J. Environ. Anal. Chem. 100 (2020) 1650–1668, https://doi.org/10.1080/03067319.2019.1657852.
[90] D.C. Montgomery, D esign and Analysis of Experiments Eighth Edition, n.d.
[91] A. Khodaii, H.F. Haghshenas, H.K. Tehrani, Effect of grading and lime content on HMA stripping using statistical methodology, Constr. Build. Mater. 34 (2012) 131–135, https://doi.org/10.1016/j.conbuildmat.2012.02.025.
[92] W. Nur, F. Wan, M.A. Ismail, H. Lee, M. Seddik, J. Kumar, M. Warid, M. Ismail, Mixture optimization of high-strength blended concrete using central composite design, 243 (2020).
[93] Y. gui Chen, L. lei Guan, S. yi Zhu, W. jia Chen, Foamed concrete containing fly ash: Properties and application to backfilling, Constr. Build. Mater. 273 (2021), https://doi.org/10.1016/j.conbuildmat.2020.121685.
[94] H. Ali, Y. Alshaeer, J.M. Irwan, A.F. Alshalif, A. Al-fakih, Review on Carbonation Study of Reinforcement Concrete Incorporating with Bacteria as Self-Healing Approach, (2022) 1–17. ⟨https://doi.org/10.3390/ma15165543⟩.
[95] Testing concrete — compressive strength of concrete cubes, (1983).
[96] E.P. Verrecchia, J. Dumont, K.E. Verrecchia, C. De Gt, L. De Pptrologie, S. Continentale, R. Tilleuls, F.- Caen, Role of calcium oxalate biomineralization by fungi in the formation of calcretes: a case study from Nazareth, Israel (2019).
[97] G. Cibilakshmi, J. Jegan, A DOE approach to optimize the strength properties of concrete incorporated with different ratios of PVA fibre and nano-Fe 2 O 3, Adv. Compos. Lett. 29 (2020), 2633366×2091388, https://doi.org/10.1177/2633366×20913882.
[98] N. Biglarijoo, M. Nili, S.M. Hosseinian, M. Razmara, Modelling and optimisation of concrete containing recycled concrete aggregate and waste glass, (2016). ⟨https://doi.org/10.1680/jmacr.16.00279⟩.

[99] M.P. Gundupalli, P. Sharma, D. Bhattacharyya, Hydrothermal Pretreatment of Tender Coconut Coir and Optimization of Process Parameters Using Response Surface Methodology (2017).
[100] A.F. Alshalif, J.M. Irwan, H.A. Tajarudin, N. Othman, A.A. Al-Gheethi, S. Shamsudin, W.A.H. Altowayti, S.A. Sabah, Factors affecting carbonation depth in foamed concrete bricks for accelerate co2 sequestration, Sustain 13 (2021), https://doi.org/10.3390/su131910999.
[101] M.S. Msebawi, Z. Leman, S. Shamsudin, S.M. Tahir, C.N. Aiza Jaafar, A.H.M. Ariff, N.I. Zahari, A. Abdellatif, Production of aluminum AA6061 hybrid nanocomposite from waste metal using hot extrusion process: strength performance and prediction by RSM and random forest, Materials (Basel) 14 (2021) 6102, https://doi.org/10.3390/ma14206102.
[102] Y. Wang, Y. Shao, M. Darko, J.K. Whalen, Recycling of switchgrass combustion ash in cement: Characteristics and pozzolanic activity with chemical accelerators, Constr. Build. Mater. 73 (2014) 472–478, https://doi.org/10.1016/j.conbuildmat.2014.09.114.
[103] C. Chandara, E. Sakai, K.A.M. Azizli, Z.A. Ahmad, S.F.S. Hashim, The effect of unburned carbon in palm oil fuel ash on fluidity of cement pastes containing superplasticizer, Constr. Build. Mater. 24 (2010) 1590–1593, https://doi.org/10.1016/j.conbuildmat.2010.02.036.
[104] A.B.H. Kueh, A.W. Razali, Y.Y. Lee, S. Hamdan, I. Yakub, N. Suhaili, Acoustical and mechanical characteristics of mortars with pineapple leaf fiber and silica aerogel infills – measurement and modeling, Mater. Today Commun. 35 (2023), 105540, https://doi.org/10.1016/j.mtcomm.2023.105540.
[105] R.S. Nampoothiri, V. Poornima, Influence of fungi: Trichoderma viride on properties of mud brick, Mater. Today Proc. 46 (2019) 5104–5111, https://doi.org/10.1016/j.matpr.2020.10.498.
[106] A.F. Alshalif, J.M. Irwan, N. Othman, A.A. Al-Gheethi, S. Shamsudin, I.M. Nasser, Optimisation of carbon dioxide sequestration into bio-foamed concrete bricks pores using Bacillus tequilensis, J. CO_2 Util. 44 (2021), 101412, https://doi.org/10.1016/j.jcou.2020.101412.
[107] M. Aziminezhad, M. Mahdikhani, M.M. Memarpour, RSM-based modeling and optimization of self-consolidating mortar to predict acceptable ranges of rheological properties, Constr. Build. Mater. 189 (2018) 1200–1213, https://doi.org/10.1016/j.conbuildmat.2018.09.019.
[108] K. Kolo, P. Claeys, In vitro formation of Ca-oxalates and the mineral glushinskite by fungal interaction with carbonate substrates and seawater, Biogeosciences 2 (2005) 277–293, https://doi.org/10.5194/bg-2-277-2005.
[109] K. Kolo, P. Claeys, In vitro formation of Ca-oxalates and the mineral glushinskite by fungal interaction with carbonate substrates and seawater, (2005) 277–293. ⟨https://doi.org/10.5194/bg-2–277-2005⟩.